AD

TR-1399

EXPERIMENTAL INVESTIGATION OF THE PERMANENT EFFECTS OF RF RADIATION IN X-BAND ON ELECTRONIC COMPONENTS

by

Nikolai Tschursin

June 1968

U.S. ARMY MATERIEL COMMAND
HARRY DIAMOND LABORATORIES
WASHINGTON, D.C. 20438

AD

AMCMS Code: 5023.11.18400
DA-1N022601A093
HDL Proj No. 24600

TR-1399

EXPERIMENTAL INVESTIGATION OF THE PERMANENT EFFECTS OF RF RADIATION IN X-BAND ON ELECTRONIC COMPONENTS

by

Nikolai Tschursin

June 1968

U.S. ARMY MATERIEL COMMAND
HARRY DIAMOND LABORATORIES
WASHINGTON, D.C 20438

A B S T R A C T

An experimental investigation was conducted at X-band frequencies to determine the effects of rf radiation on composition resistors, crystal diodes, transistors, and metal oxide silicon field-effect transistors (MOSFET). To obtain maximum power transfer, the component leads were cut and bent to form a half-wave dipole tuned to the excitation frequency. The component was placed in a microwave assembly, oriented parallel to the electric field, and exposed for several minutes until thermal equilibrium was established.

Data concerning permanent changes in the electrical characteristics of the components as a function of exposure to the E-field were obtained. Measurements were taken of the temperature rise of the components while various types of convection and forced-air cooling were employed. These measurements indicate that the changes in the electrical characteristics of the components are primarily a function only of the temperature rise produced in the component and only secondarily, if at all, a function of the field intensity per se.

CONTENTS

ILLUSTRATIONS

I L L U S T R A T I O N S—Cont'd

I L L U S T R A T I O N S—Cont'd

BLANK PAGE

1. INTRODUCTION

HDL has been investigating the effects of rf energy on components used in the initiating circuits of fuzes. Hazardous conditions may exist when such devices are placed in strong rf fields, such as those produced by radars or communication transmitters. Normally, fuze components are protected from the undesired direct rf radiation by a shielded inclosure, but in some cases the external connecting wires may serve as a coupling mechanism between the irradiating rf field and the circuit, because of pickup in the wiring or inadequate shielding. The fields may cause prefunction of a fuze or permanent changes in the electrical characteristics of the components, which may affect its reliability.

The present experimental investigation was conducted in X-band. The intention was to determine only the minimum rf field strength which, under long exposure, causes permanent changes in the electrical characteristics of the components. No attempt was made to determine whether the exposure was realistic of conditions in the field.

Knowledge of the threshold field affecting the components will allow determination of shielding protection required in a hazardous environment.

2. GENERAL DISCUSSION

If a component is placed in an rf field so that two of its leads form a dipole, the power transferred to the component will depend on:

(a) Orientation of the dipole relative to the E-field,

(b) Impedance of the load connected to the terminals of the dipole,

(c) Field strength, and

(d) Wavelength.

If certain simplifying assumptions are made, the power absorbed by the component can be calculated. It is assumed that:

(a) The component is placed in the field with its leads parallel to the E-field;

(b) The leads form a thin half-wave dipole tuned to resonance;

(c) The load impedance of the component is the complex conjugate of the half-wave dipole radiation impedance, whose resistive component is equal to 80 Ω (approx);

(d) The effective length ℓ of the half-wave dipole is λ/π.

The power into the load can be expressed as

$$P = \frac{V_o^2 Z_L}{(Z_L + Z_o)^2} \qquad (1)$$

where

P = power into the load (W)

V_o = open-circuit voltage at the dipole terminals (V)

Z_L = load impedance (Ω)

Z_o = dipole radiation impedance (Ω)

If Z_L is the complex conjugate of Z_o, the expression becomes

$$P = \frac{V_o^2}{4 R_L} \qquad (2)$$

where

R_L = real part of $Z_L \cong 80\ \Omega$

Now,

$$V_o = E\ell$$

where

E = electric field intensity (V/m), and

ℓ = effective length of the half-wave dipole (m).

Substituting, we have

$$P = \frac{E^2 \ell^2}{4 R_L} = \frac{E^2 \lambda^2}{4 \times 80 \times \pi^2} \text{ watts} \qquad (3)$$

$$P = E^2 \lambda^2\ 3.16 \times 10^{-4} \text{ watts}$$

If, for example,

λ = 4 cm

E = 1000 V/m

then,

P = 0.5 W

The value of the power absorbed by the actual components tested cannot be easily computed since the simplifying assumptions do not

necessarily apply. However, to obtain maximum power transfer in the present experiments, the leads of each component were cut to form a dipole and the component was placed in the rf field with its leads parallel to the E-field. Experimental data, described in section 5, show reasonably good agreement with the results obtained from this idealized model

3. DESCRIPTION OF EXPERIMENTAL SETUP

Preliminary investigations of the rf susceptibility of electronic components revealed that fields of several hundred volts per meter produced no observable effect on the components tested. A stronger rf field was needed. A simple setup was therefore constructed to produce fields of several thousand volts per meter and allow an investigation of the effect of X-band rf fields on small electronic components. Figure 1 is a block diagram and figure 2 is a photograph of the bench setup.[1] A Hewlett Packard (HP) SHF signal generator (model 620-A) with an output of 1 mW over a 7- to 11-GHz range was connected to an Alfred microwave TWT amplifier (model 527-S1) capable of producing 10 W. A Ferrotec isolator (model 1-155 L) with 1-dB attenuation in the forward direction and about 20 dB in the reverse direction were used to prevent reflected energy from returning to the amplifier. The output from the amplifier was connected to the following X-band waveguide equipment: two 20-dB directional couplers (HP model X752D) with HP model X382-A variable attenuators. HP model 431-B power meters were used to measure the input and reflected power. The microwave energy was then fed to a specially constructed microwave assembly (fig. 3), which consisted of a Waveline-type 683 tuner and two X-band horn antennas hinged so that the second horn could be placed to intercept all energy radiated by the first. The upper horn can be connected through a piece of waveguide to a high-power variable attenuator HP model X382-A and HP power meter, model 431-B, or to a variable short. To facilitate monitoring the field in the horn, a probe made from an X-band slotted-line probe unit was installed in the wall of the horn. The dimensions of the horn were chosen to reduce the possibility of generating higher order modes. The width of the horn is the same as the width of the X-band waveguide (2.3 cm), and the height flares out to a maximum of 4 cm. The component to be irradiated, supported by a piece of fiberglass, is placed in the horn so that the two leads form a dipole parallel to the E-field in the center of the horn. Thermocouple wires enter the horn through a small opening near the fiberglass support.

4. DETERMINATION OF FIELD INTENSITY

Exact determination of field intensity in the horn when a component is placed in it is difficult because of the scattering of EM waves by the component and leads. However, the field-intensity

[1] Illustrations appear on pages 22 through 65.

distribution in the horn when the component is not present and the horn is radiating into free space can be computed as a function of power into the horn and its geometry. Under these conditions the reflected power was measured to be less than 5 percent of the transmitted power. The component is placed in the horn as shown in figure 4. The E-field is parallel to the component leads and side b.

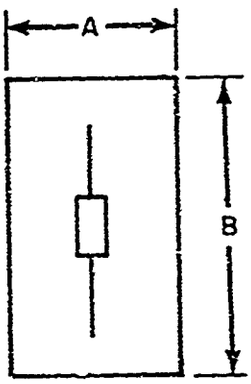

a = 0.023 m

b = 0.038 m

ab = cross-sectional area perpendicular to the direction of propagation of the wave

$= 0.023 \times 0.038 \times 10^{-4} m^2$

Figure 4. Diagram of component in horn.

The electric field in the TE_{10} mode has a sinusoidal distribution across side a, being greatest in the center where the component is located, and zero at the edges. Its value in the center is (ref 1):

$$E = V/b, \tag{4}$$

where V = the rms voltage across the waveguide. For this mode, for a nondissipative guide (ref 2),

$$V = \sqrt{P}\,\sqrt{\lambda_G/\lambda}\,\sqrt{2b/a}\,\sqrt{\zeta} \tag{5}$$

where

ζ = impedance of free space = 377 Ω

P = power input in watts

λ = wavelength in free space

$\lambda_G = \dfrac{\lambda}{\sqrt{1 - (\lambda/2a)^2}}$ "The guide wavelength" (ref 3).

For

$\lambda = 3.10^{-2}$ meters

and $a = 2.3 \times 10^{-2}$ meters,

$\lambda_G = 3.97 \times 10^{-2}$ meters (6)

Substituting, we have

$$E = 1070\sqrt{P} \approx 1000\sqrt{P} \qquad (7)$$

To monitor the actual E-field at the component, a probe was installed in wall a of the horn parallel to the E-field and coaxial with the leads of the component. An X-band slotted-line probe unit was used. It was connected to a coaxial thermistor mount and an HP model 478-A used with HP model 431-B power meter. The power picked up by the probe P_C was noted for a field intensity E_C, computed using equation (7) and a known power into the horn. The probe, thus calibrated, can be used to determine the field opposite it under any conditions with the use of the formula

$$E = \sqrt{P_P / P_C}\ E_C$$

where P_p is the probe power under the new conditions. The probe indicated that the presence of the component in the horn lowered the actual value of the field intensity by scattering the EM wave and possibly the input power.

The rf amplifier used in this investigation can produce up to 10-W rf power, which will allow generation of undisturbed fields up to 3000 V/m at the location of the tested component. This value of field intensity can be increased by terminating the power radiating horn with another horn and a variable length of shorted waveguide. If the short is $n\lambda/2 + \lambda/4$ (where n is an integer) away from the component, the field intensity will be twice the value that it was without the short, assuming that the reflected wave is absorbed by the generator. The presence of multiple reflections in the horn caused a deviation from this value. However, if the probe is calibrated with the horn terminated by space (that is, negligible reflection) and with no component present, it will give the true value of the field intensity in the vicinity of the component even if there are multiple reflections.

5. DETERMINATION OF POWER ABSORBED BY COMPONENT

A simple mathematical model was used to determine the power absorbed by the component when exposed to rf radiation. The rf power supplied to the horn is dissipated in the following four ways:

$P_{absorbed}$ -- Power absorbed by the component placed in the horn.

$P_{dissipated}$ -- Power picked up by the second horn and dissipated in the high power variable attenuator.

$P_{reflected}$ -- Power reflected back into the waveguide.

P_{lost} -- Power absorbed in waveguide, radiated through leaks and otherwise unaccounted for.

The power equation can be expressed as:

$$P_{input} = P_{absorbed} + P_{dissipated} + P_{reflected} + P_{lost}. \quad (8)$$

The power losses in the system can be determined when the tested component is not present, since P_{input}, $P_{dissipated}$, and $P_{reflected}$ are measurable (fig. 1).

$$P_{lost} = P_{input} - P_{dissipated} + P_{reflected}. \quad (9)$$

If it is assumed that the value of the power lost does not change appreciably when the component is placed in the horn, the value of the power absorbed can be determined as follows:

$$P_{absorbed} = P_{input} - P_{dissipated} + P_{reflected} + P_{lost} \quad (10)$$

where P_{lost} was previously determined.

The experimental data of the power absorbed by the component obtained by this method show a good agreement with the equation (3) derived in section 2 for an idealized model. This is illustrated in figures 36 through 39 where the values of the absorbed power are indicated for different values of field intensity generated in the horn. At high values of the field intensity, the agreement with equation (3) is not as good as it is at low values, which may be because of a greater impedance mismatch caused by higher temperatures developed in the components with increased field. For example, 0.5 W is absorbed in a field of 1000 V/m and 1.0 W in fields of 1600 V/m and 1800 V/m. At these levels, the agreement with equation (3) is within 25 percent. However, 1.8 W is absorbed in a field of 2500 V/m and 2.75 W in a field of 3000 V/m; and at these levels, the agreement is only within 50 percent.

6. DETERMINATION OF TEMPERATURE OF COMPONENT

To observe temperature changes in the component during exposure to rf radiation, a Chromel-Alumel thermocouple was used. The thermocouple junction was welded to a small copper sleeve with dimensions that allowed ample thermal contact, and easy insertion and removal of the component's lead. The sleeve was permanently mounted on a piece of fiberglass placed in the horn perpendicular to the E-field. The thermocouple junction measures the temperature of the lead where it enters the component. The thermocouple wires enter the horn through a small opening, approach the component perpendicular to the E-field, and do not appreciably disturb the field. The other ends of the thermocouple wires are connected to a high-sensitivity recorder. The voltage between the thermocouple wires is closely proportional to

the temperature difference between the recorder terminals and the junction. Standard NBS tables for thermocouples (ref 4) were used to convert the thermocouple voltages to equivalent temperatures.

7. RESISTOR MEASUREMENTS

Quarter-watt composition resistors were individually placed in the above-described microwave assembly (fig. 3) and exposed to rf radiation. The leads of the resistors were cut to about 1/4 wavelength (guide wavelength) and the frequency of the radiation was tuned to achieve maximum coupling. The leads were parallel to the E-field. A thermocouple junction was attached to one of the leads as described above. Since the temperature of the resistors increases monotonically with absorbed power, the voltage output from the thermocouple, in addition to indicating the temperature, served as a convenient device to indicate maximum coupling. Figures 5 through 9 show normalized resistance measured after the resistors were exposed to rf radiation of the indicated field intensity for 10 min, both with and without forced-air cooling. Curves of equilibrium temperature measured during the exposure to rf radiation are also shown for each nominal value of resistor, both for forced-air cooling and for cooling by convection only. The shaded portions of the curves represent the spread for about 90 percent of all measurements. The density of the distribution of the values is not uniform; values of normalized resistance larger than 2 occurred only in 10 percent of the samples. Some 40 to 60 resistors of each nominal value were tested. As is shown in the graph, the threshold field intensity causing permanent change in the resistance of resistors that were not forced-air cooled varied from 1300 V/m for 2-kΩ resistors to 1650 V/m for 2-MΩ resistors, corresponding to a temperature of about 120°C in each case. Above about 200°C, a permanent sharp drop in resistance took place. However, field intensities up to 2000 V/m caused no permanent changes in the resistors that were forced-air cooled.

Measurements of the value of the power absorbed by resistors of various nominal values exposed to the same field intensity indicated that maximum coupling was slightly greater for the 200-Ω and 2-kΩ resistors, and somewhat less for 2-MΩ resistors than that for the other values. The experimental data indicate that the permanent change in resistors after exposure to rf radiation is a function only of the temperature the resistor reaches; that is, the field intensity needed to cause a given change in a resistor depends not only upon the coupling but on the heat dissipation capabilities of the resistor.

8. DIODE MEASUREMENTS

Several types of silicon and germanium diodes were exposed to rf radiation in the microwave assembly, using techniques described in section 7. Figures 10 through 17 and 20 through 24 show typical forward and reverse electrical characteristics of some of the tested diodes before and after exposure to field intensities of the indicated values. The temperature rise in the diodes is also shown as measured by the thermocouple during the exposure, both with and without forced-air cooling.

8.1 Germanium Diodes

As is illustrated in figures 10 and 11, 1N67-A germanium diodes that were cooled by convection became short circuited upon exposure to fields of 3000 V/m at the time the temperature reached 160°C. The diodes that were forced-air cooled (fig. 12) experienced only a moderate change upon exposure to field intensities up to 4000 V/m when their temperature reached about 100°C. This comparison reveals that the change in the electrical characteristics of the diode is a function of the temperature rise and not of the field intensity. The rate of heat dissipation from the diode determines the value of the field intensity needed to cause a given change in the electrical characteristics.

To examine the effect of the thermocouple on the diode lead, tests were run without the thermocouple on about 30 diodes, but otherwise identical with the diode tests under convection cooling. Several typical sets of test results are shown in figures 13 to 17. Comparison with figures 10 and 11 shows that rf fields cause no greater effect on diodes without thermocouples than on diodes with them. Figures 18 and 19 show changes in the normalized forward and reverse currents of the 1N67-A germanium diode after exposure to the indicated field intensities with heat dissipation by convection only. The forward current was measured at +0.6 V and the reverse current at -60 V. The shaded area of the curves represents the spread in the value of normalized current among the central 90 percent of all measured samples. An examination was made with 40 to 50 diodes of this type. The curve within the shaded area (fig. 18,19) gives the change in the current for a typical diode. Exposure to field intensities up to 600 V/m for several minutes caused no observable change in the characteristics of the diode. After exposure to fields between 600 and 2000 V/m, both forward and reverse currents increased in most of the samples. For exposure to field intensities between 2000 and 3000 V/m, a drop in forward current and a sharp increase in reverse current were noted in most samples. Exposure to field intensities above 3000 V/m shorted the diodes.

8.2 Silicon Diodes

Figures 20 through 22 show the effect of exposure to EMR on three different samples of 1N3066 silicon diodes. Exposure to field intensities up to 3000 V/m caused a temperature rise to 260°C but no observable change in the electrical characteristics in any of the samples. However, 3500 V/m raised the temperature of one diode to 270°C and also caused it to open up; 4000 V/m in the second diode caused a temperature rise to 300°C and changed the reverse breakdown voltage from 160 to 15 V, and 4000 V/m in the third sample raised the temperature to 280°C but produced no change. One sample of the HP2201 silicon "hot-carrier" diode was tested and the results indicated that the exposure to field intensities of 2000 V/m caused the temperature to rise to 150°C and change in the electrical characteristics as shown in figure 23.

Exposure to field intensities of 4000 V/m had no effect on the electrical characteristics of 1N747-A silicon diodes (fig. 24). One of the five diodes of this type tested was found to be open circuited after exposure to 2000 V/m. However, it is suspected that accidentally applied high voltage from the transistor curve tracer instead of rf energy caused its destruction.

On the basis of these experiments, it can be concluded that higher temperatures are required to cause changes in the electrical characteristics of silicon diodes than are required to cause changes in germanium diodes. As was concluded in the case of germanium diodes, temperature rather than field strength is the determining factor in producing permanent changes in silicon diode characteristics.

9. TRANSISTOR MEASUREMENTS

Sikora and Miller (ref 5) report on the failure of a transistor as a function of the junction temperature of the transistor. They show that although different failure mechanisms are stimulated by different types of stress, the rate of device failure is still determined by the junction temperature of the device. Peterman (ref 6) examines the temperature distribution over the active area of silicon transistors and reports that there is a different distribution of temperatures for various values of I_c and V_{ce} when holding the product ($I_c \cdot V_{ce}$) constant. He observes that the formation of hot spots at the junction was responsible for the damage to the transistors, and points out the difficulty in defining junction temperature uniquely.

Types 2N3785 (germanium) and 2N2714 (silicon) transistors were utilized in the investigation of the effects of rf radiation on transistors. As with resistors and diodes, the transistors were

placed individually in the microwave assembly and exposed to known rf fields in X-band. The base and emitter leads were bent and cut to form a half-wave dipole oriented parallel to the E-field.

Measurements of the junction temperature of the transistors exposed to rf radiation were not attempted in view of the earlier findings. However, case temperature measurements were obtained by a thermocouple attached to the case lead (2N3785) or collector lead (2N2714).

Figures 25 through 34 show the collector characteristics of typical transistors obtained before and after exposure to electric fields. Figures 25 through 30 also indicate the temperatures reached by the transistors during their exposure when heat dissipation was by convection only. Figures 31 and 32 show the temperatures when transistors were cooled by forced air during the exposure. Figures 33 and 34 show the electrical characteristics of the transistors after exposure without forced-air cooling and with no thermocouple attached. Forced-air cooling had the same effect as that observed with resistors and diodes—that is, higher field intensities were needed to cause equivalent changes in the electrical characteristics with forced-air cooling than with convection cooling.

Figure 35 shows results of the investigation with 47 2N3785 germanium and 63 2N2714 silicon transistors that were cooled by convection. Curves 1A and 2A show the cumulative distribution, expressed as a percentage of the respective populations of the transistors whose a-c betas changed more than 20 percent from their original values, plotted against the electric field causing the beta change. Curves 1B and 2B show the distribution of germanium and silicon transistors that experienced catastrophic failure. Temperatures reached by both transistor types are also plotted against the field strength in curves 1C and 2C. The temperature data are the means of all recorded measurements of temperature versus electric field for each transistor type. It can be seen that no transistors, germanium or silicon, were affected by exposure for several minutes to fields below 600 V/m. Fields of 900 V/m caused catastrophic failure in about 50 percent of germanium transistors, and fields of 1000 V/m caused catastrophic failure in about 50 percent of all silicon transistors. About 115°C was recorded for germanium and 180°C for silicon transistors before catastrophic failure occurred in half the respective populations.

10. MOSFET MEASUREMENTS

Metal oxide silicon field-effect transistors (MOSFET) in two different case sizes (TO-5, TO-46), with the same electrical characteristics, were examined to determine the relation between their

thermal capacity and the field intensity causing permanent changes. The TO-5 is 0.35 in. (9 mm) in diameter and 0.18 in. (4.5 mm) high, while the TO-46 is 0.22 in. (5.5 mm) in diameter and 0.08 in. (2 mm) high. The source and gate leads were cut and bent to form a half-wave dipole oriented parallel to the E-field. The MOSFET's were individually placed in the microwave assembly and exposed to known rf fields in X-band in the manner described previously.

Figures 36 through 39 show the drain characteristics of typical 2N3608 MOSFET's of both case sizes obtained before and after exposure to electric fields of indicated values while cooled by convection. The power absorbed by the MOSFET's after thermal equilibrium was reached is also indicated. The lower curves show the temperature of the MOSFET's measured with the thermocouple on the case lead during exposure to the indicated field intensities. Figure 40 shows the drain characteristics and the temperature curves of the 2N3608 MOSFET (case size TO-46) with forced-air cooling. Figure 41 shows the normalized transconductance of the MOSFET against applied rf field intensity for various mounting configurations having different thermal capacities.

These figures illustrate that when the thermal capacity was decreased (that is, smaller case or no case), less field intensity and less absorbed power were required by the MOSFET to cause changes in its electrical characteristics. When the thermal capacity was increased by cooling the MOSFET with the blower as it was exposed to rf radiation, the required field intensity and absorbed power also were increased.

The thermal capacity of a MOSFET depends on the area of its case since heat dissipation is mainly by convection. The powers absorbed by the two sizes of MOSFET's that caused identical changes in their electrical characteristics were proportional to the ratio of the heat-dissipating areas of their cases.

These measurements give a convenient indication of the temperature variation with power absorbed by the MOSFET. It was observed that identical changes in the electrical characteristics of all tested samples of the same size case occurred at the same case equilibrium temperature, suggesting that—as is the case with d-c heating (sect 10.1 and ref 5)—the failure of MOSFET's when exposed to rf heating is only a function of the temperature reached.

10.1 D-C Heating

Measurements were taken to compare the values of d-c and rf power needed to cause changes in the case temperature and in the electrical characteristics of the MOSFET's. Figures 42 and 43 show that the same d-c power was required to cause changes in the electrical characteristics of the MOSFET's for both case sizes. This

value was much less than the value of rf power required to cause the same changes.

10.2 Oven Heating

MOSFET's were heated in an oven and drain characteristics were obtained for various temperatures as shown in figure 44. The drain characteristics were also obtained after the MOSFET's were removed from the oven and allowed to cool to room temperature. A slight change in the value of the transconductance was noted after heating to 350°C and cooling to room temperature. Heating to 420°C and cooling to room temperature caused the transconductance to change to 50 percent of the initial value, and heating to 520°C caused complete and permanent destruction of the MOSFET.

11. CONCLUSIONS

Data concerning permanent changes in the electrical characteristics of the investigated components as a function of exposure to the E-field indicate that the changes are predominantly due to the temperature rise produced in the component by the field. The field intensity, per se, has little if any effect on the components tested. Consequently, the ability of a component to dissipate heat must be considered at least as important as the strength of the electromagnetic field to which the component is exposed.

12. LITERATURE CITED

(1) Marcuvitz, N., "Waveguide Handbook," p. 62, MIT Rad. Lab Series. v. 10, New York, McGraw Hill, 1951.

(2) Ibid, p. 62.

(3) Ibid, p. 62, eq 14b.

(4) Shenker, Rouritzen, Corruccini and Bonberger, "Reference Tables for Thermocouples," p. 23, NBS Circular 561, Washington, D. C., 27 Apr 1955.

(5) Silora, G. C. and Miller, L. E., "Application of Power Step Stress Techniques to Transistor Life Predictions," Physics of Failure in Electronics, v. 3, p. 30.

(6) Peterman, D. A., "Thermophysics of Silicon Power Transistors," Physics of Failure in Electronics, v. 4. p. 279.

ACKNOWLEDGEMENT

The author gratefully acknowledges the many helpful discussions and insights offered by HDL staff members E. Ramos, J. C. Lowe, J. A. Rosado, and NASA staff member V. Danchenko.

* * *

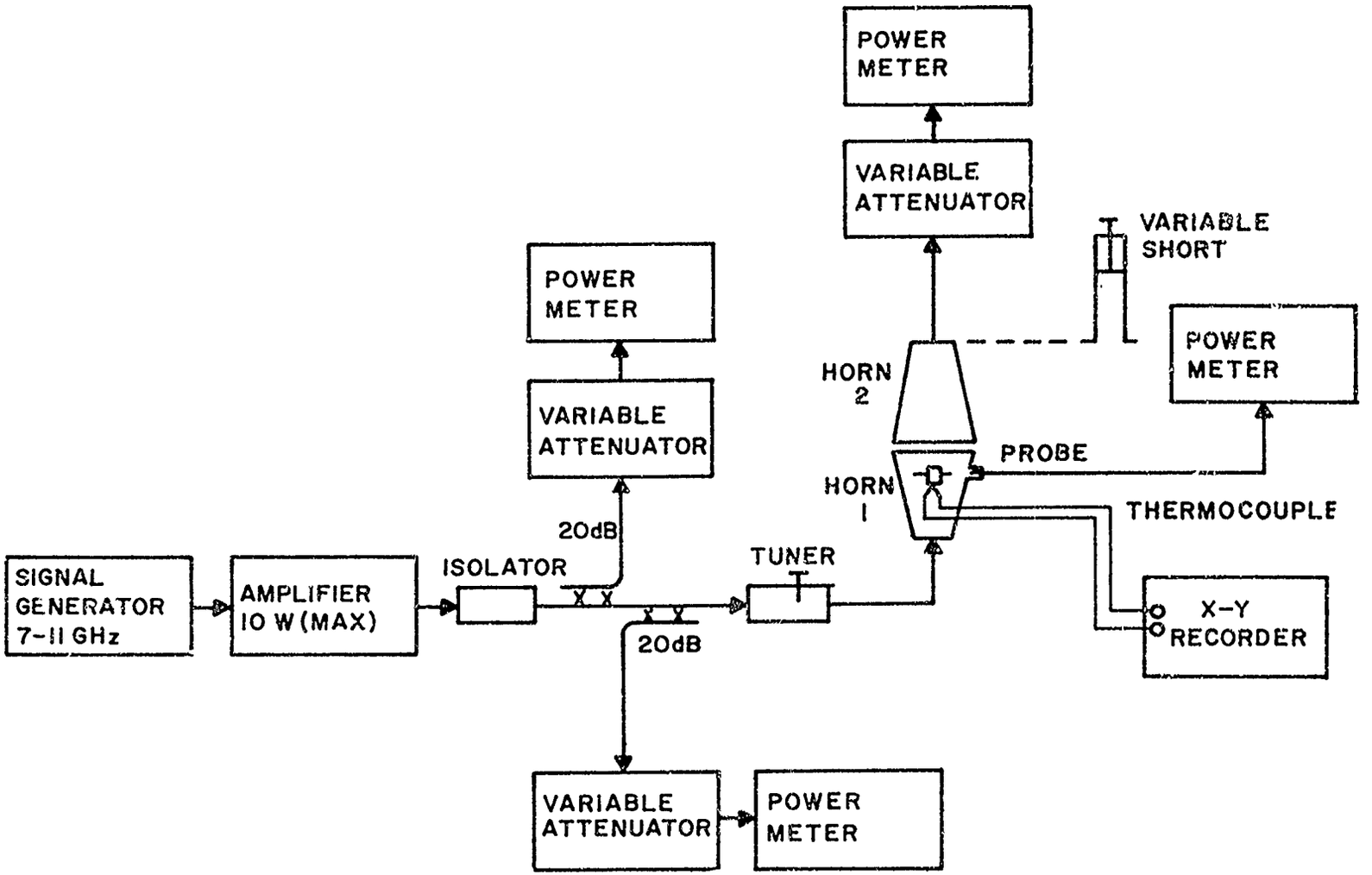

Figure 1. Block diagram of setup used for measuring the effects of rf power radiation on electronic components.

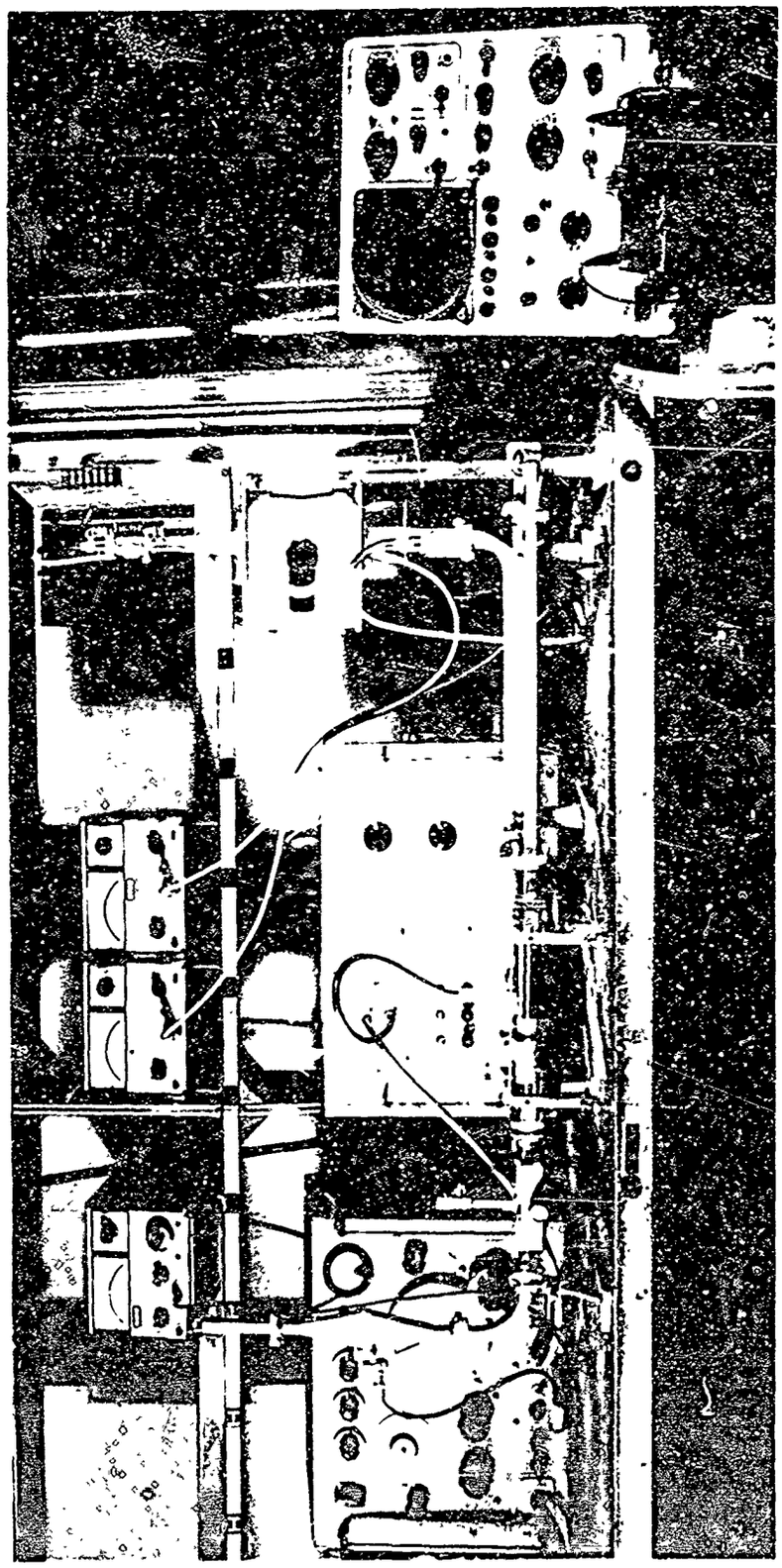

Figure 2. Test setup.

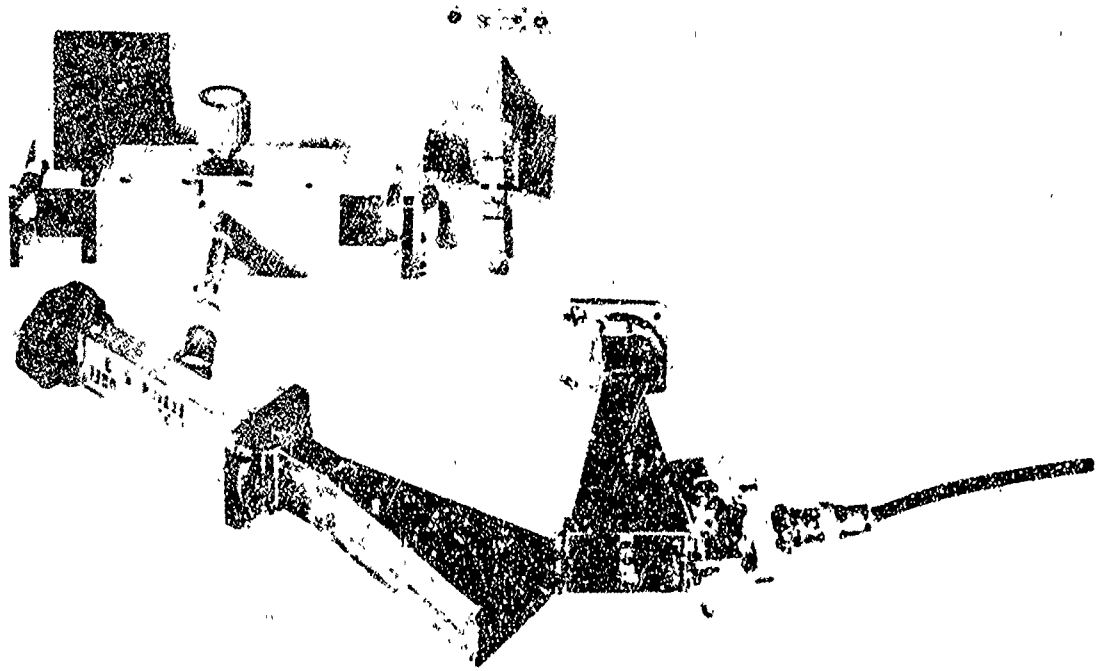

Figure 3. X-band rf radiation assembly.

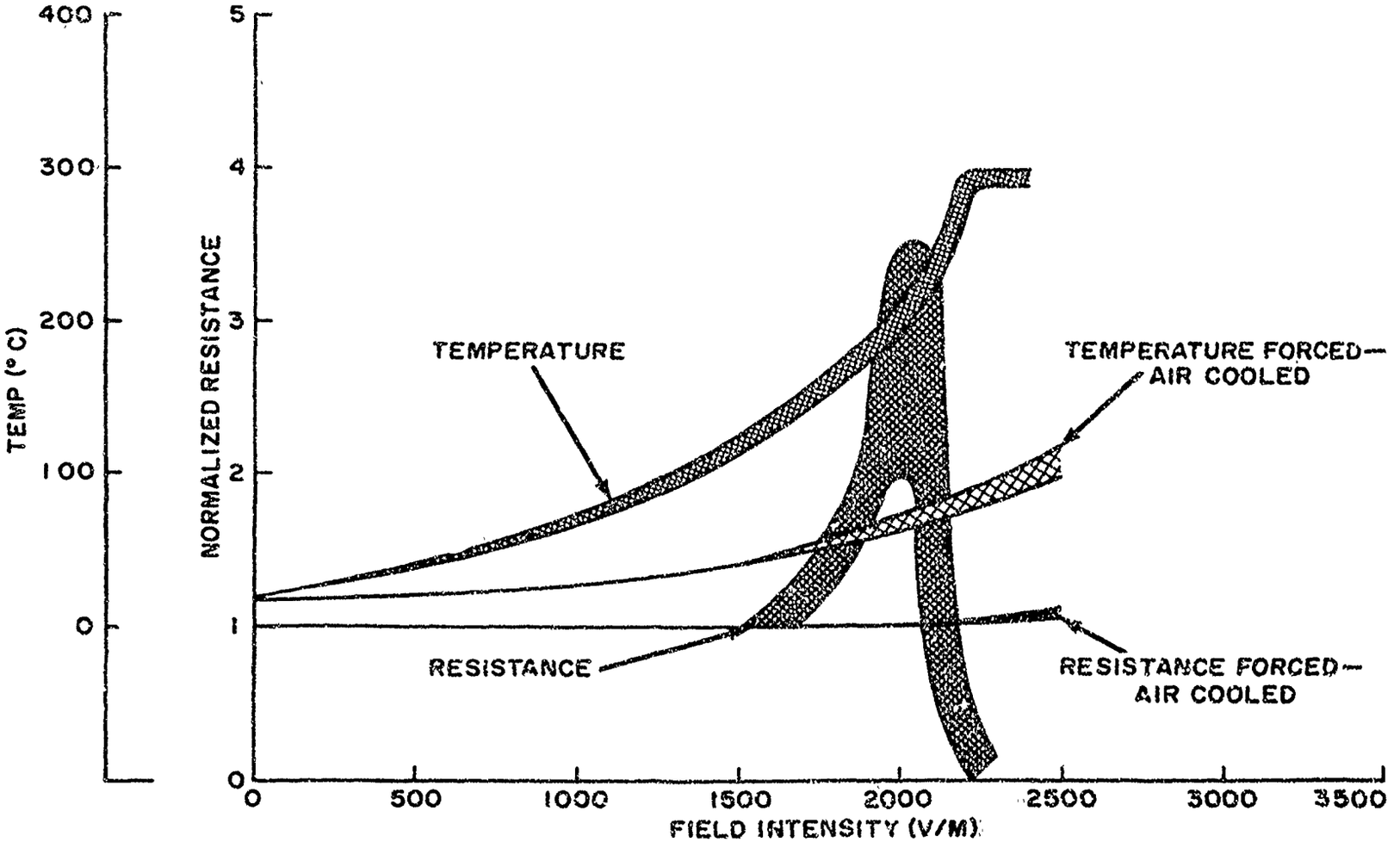

Figure 5. Effect of EMR on 1/4-W composition resistors—nominal value of resistor 2 MΩ.

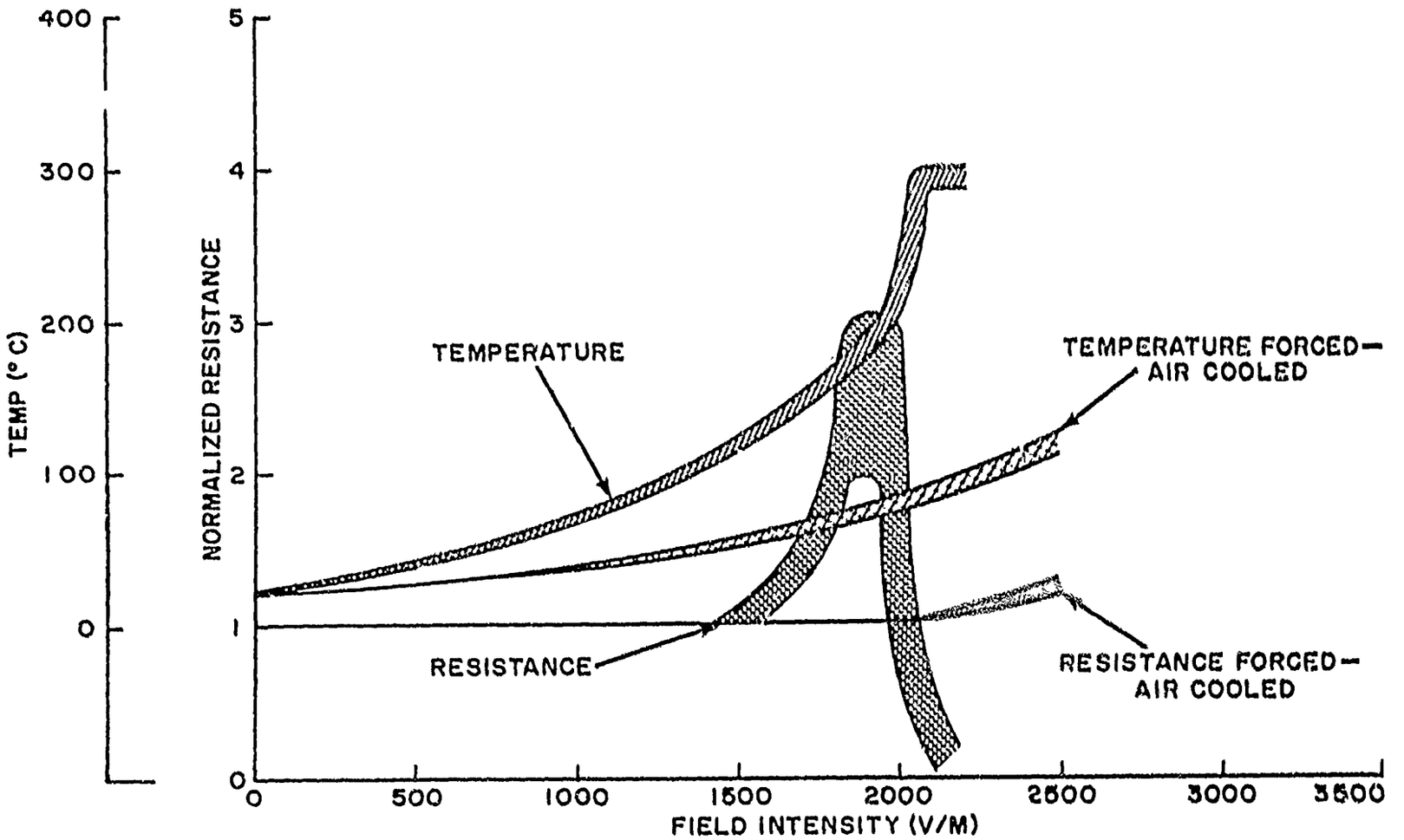

Figure 6. Effect of EMR on 1/4-W composition resistors—nominal value of resistor 200 kohms.

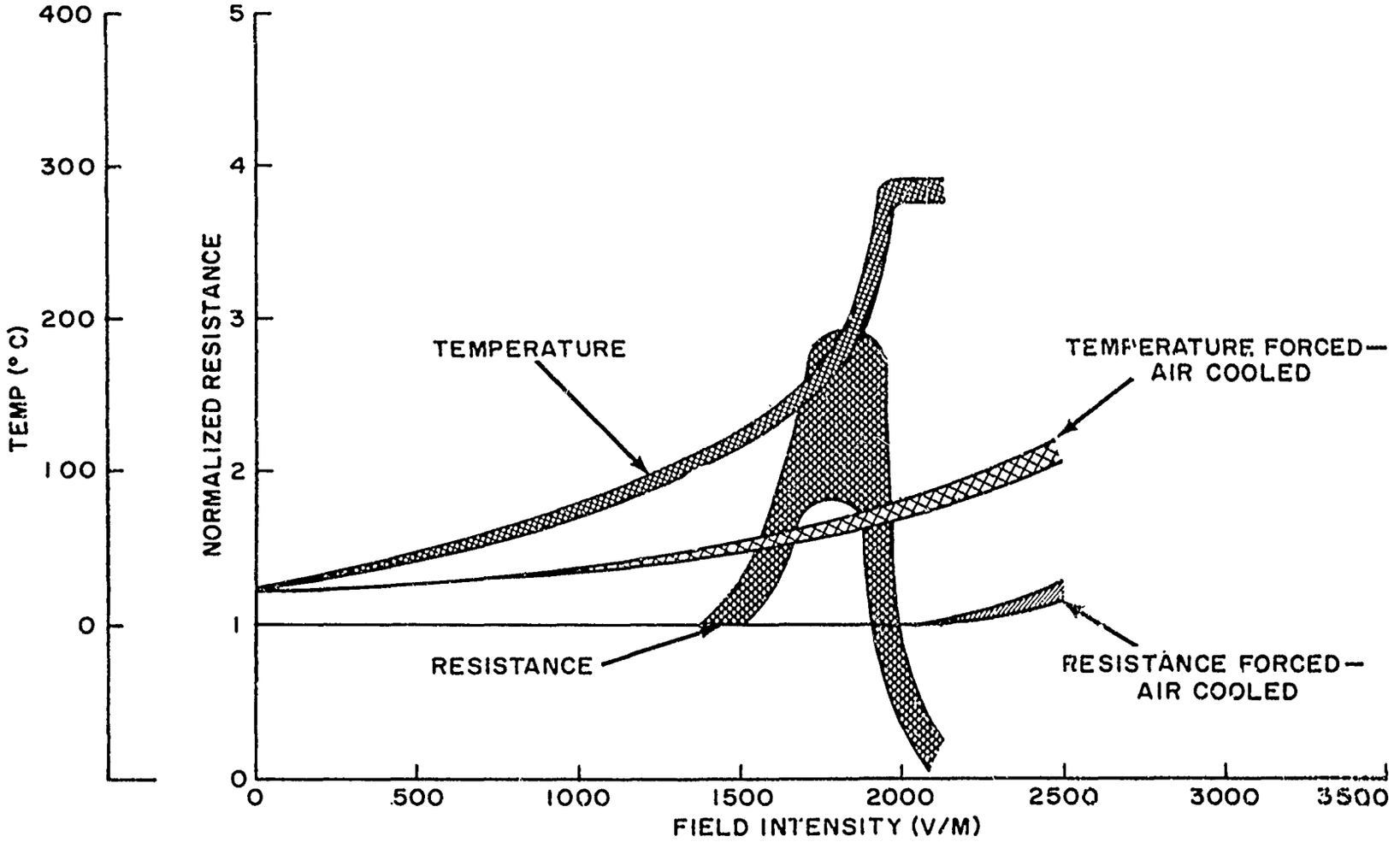

Figure 7. Effect of EMR on 1/4-W composition resistors—nominal value of resistor 20 kohms.

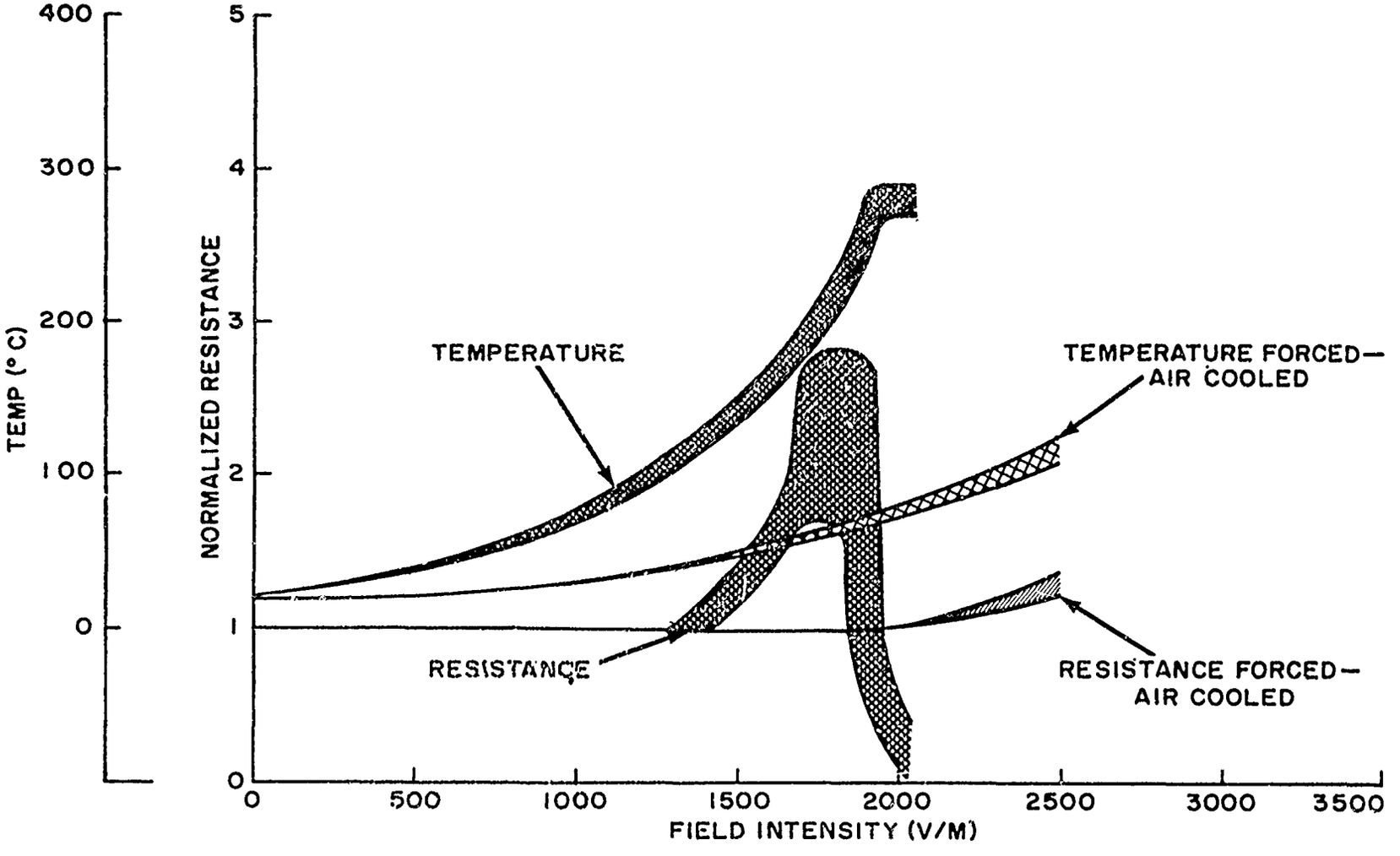

Figure 8. Effect of EMR on 1/4-W composition resistors—nominal value of resistor 2 kohms.

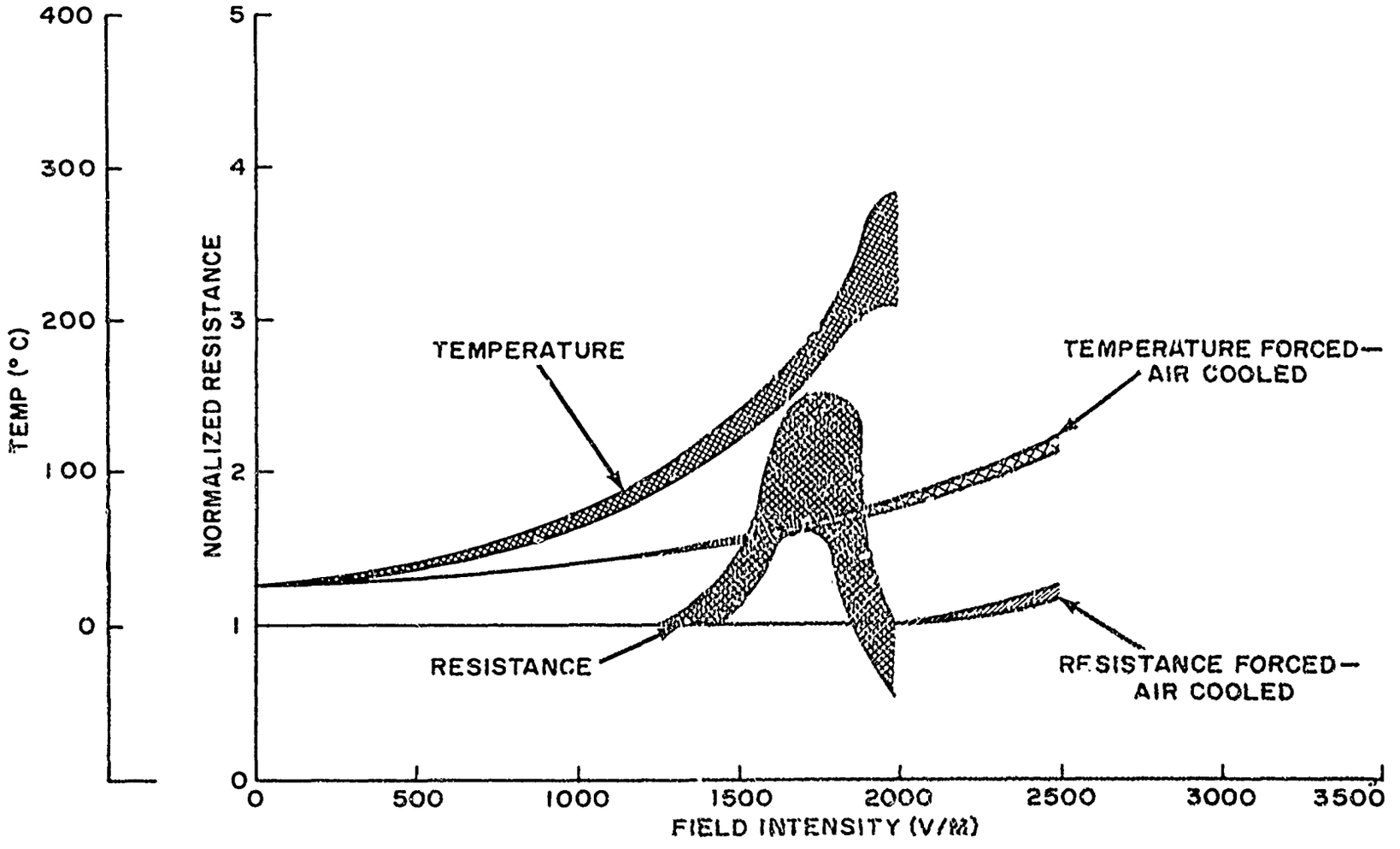

Figure 9. Effect of EMR on 1/4-W composition resistors—nominal value of resistor 200 Ω.

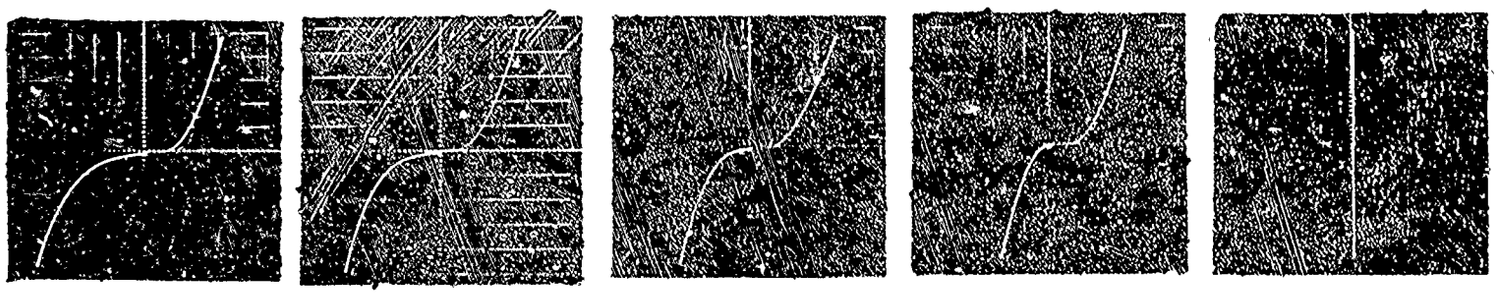

0.0 V/m 1500 V/m 2000 V/m 2500 V/m 3000 V/m

FORWARD AND REVERSE CHARACTERISTICS OBTAINED AFTER EXPOSURE TO FIELD INTENSITIES OF INDICATED VALUES. VERTICAL SCALE FOR THE FORWARD CHARACTERISTICS: 1.0 mA/DIV; FOR THE REVERSE CHARACTERISTICS: 0.02 mA/DIV. HORIZONTAL SCALE FOR THE FORWARD CHARACTERISTICS: 0.2 V/DIV; FOR THE REVERSE CHARACTERISTICS; 20 V/DIV.

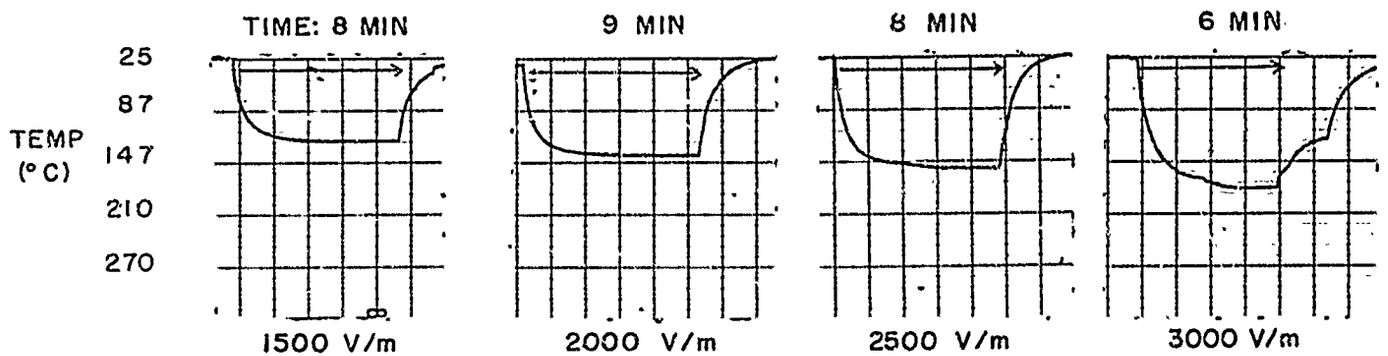

TEMPERATURE OF THE DIODE MEASURED AT THE CATHODE LEAD AS THE DIODE WAS EXPOSED TO rf RADIATION OF INDICATED FIELD INTENSITIES.

Figure 10. Electrical characteristics of 1N67-A germanium diode after exposure to EMR—cooled by convection.

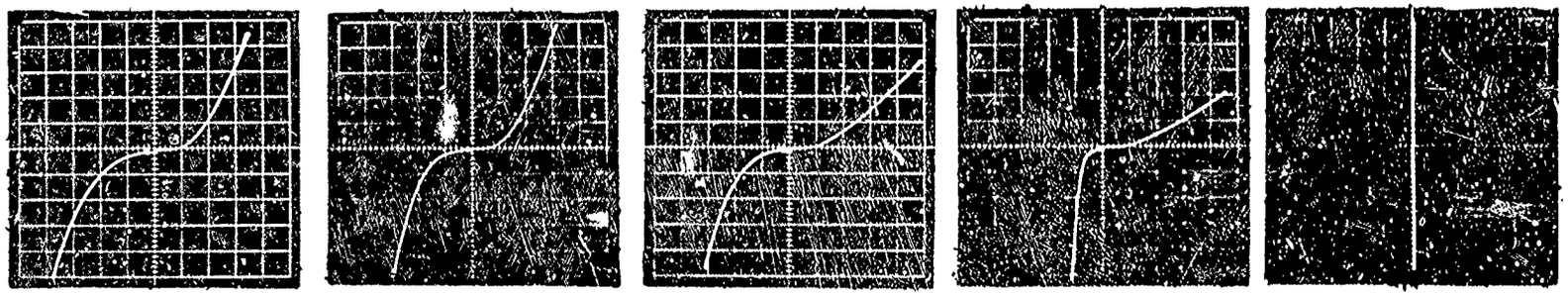

0.0 V/m 1000 V/m 1500 V/m 2500 V/m 3000 V/m

FORWARD AND REVERSE CHARACTERISTICS OBTAINED AFTER EXPOSURE TO FIELD INTENSITIES OF INDICATED VALUES. VERTICAL SCALE FOR THE FORWARD CHARACTERISTICS: 1.0 mA/DIV; FOR THE REVERSE CHARACTERISTICS: 0.02 mA/DIV. HORIZONTAL SCALE FOR THE FORWARD CHARACTERISTICS: 0.2 V/DIV; FOR THE REVERSE CHARACTERISTICS; 20 V/DIV.

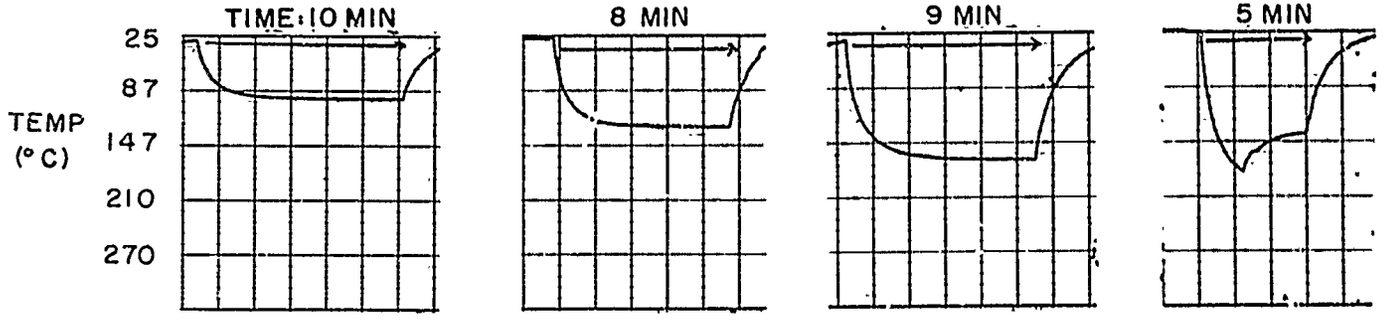

TEMPERATURE OF THE DIODE MEASURED AT THE CATHODE LEAD AS THE DIODE WAS EXPOSED TO rf RADIATION OF INDICATED FIELD INTENSITIES.

Figure 11. Electrical characteristics of 1N67-A germanium diode after exposure to EMR—cooled by convection.

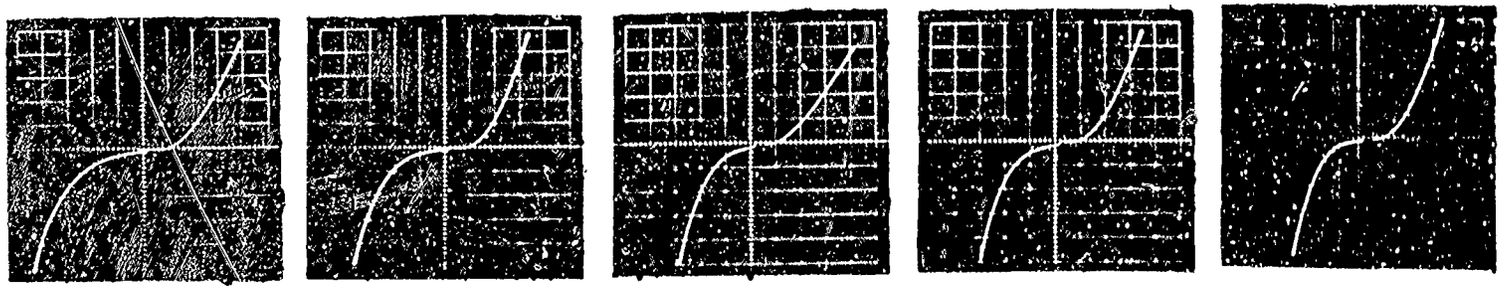

0.0 V/m 1000 V/m 2000 V/m 3000V/m 4000 V/m

FORWARD AND REVERSE CHARACTERISTICS OBTAINED AFTER EXPOSURE TO FIELD INTENSITIES OF INDICATED VALUES. VERTICAL SCALE FOR THE FORWARD CHARACTERISTICS: 1.0 mA/DIV; FOR THE REVERSE CHARACTERISTICS; 0.02 mA/DIV. HORIZONTAL SCALE FOR THE FORWARD CHARACTERISTICS: 0.2 V/DIV; FOR THE REVERSE CHARACTERISTICS; 20 V/DIV

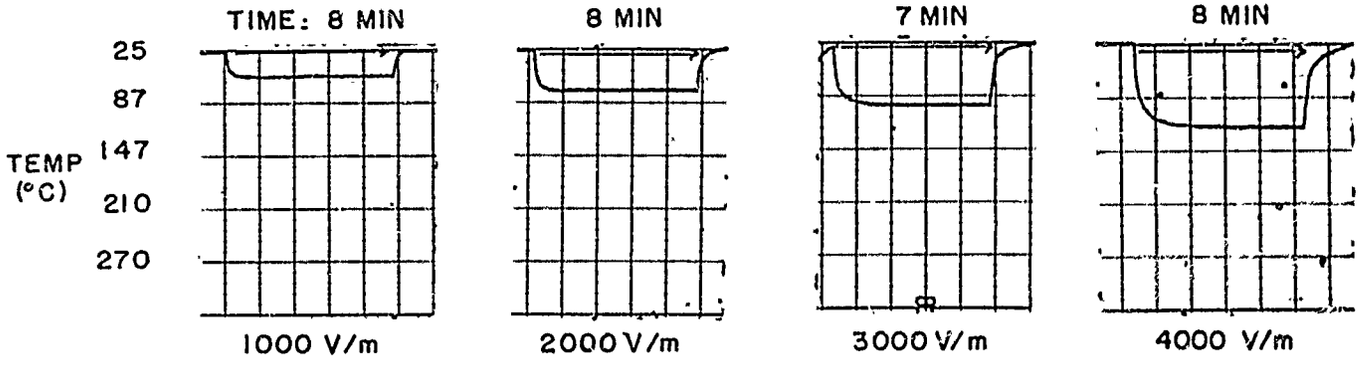

TEMPERATURE OF THE DIODE MEASURED AT THE CATHODE LEAD AS THE DIODE WAS EXPOSED TO rf RADIATION OF INDICATED FIELD INTENSITIES.

Figure 12. Electrical characteristics of 1N67-A germanium diode after exposure to EMR—forced-air cooled.

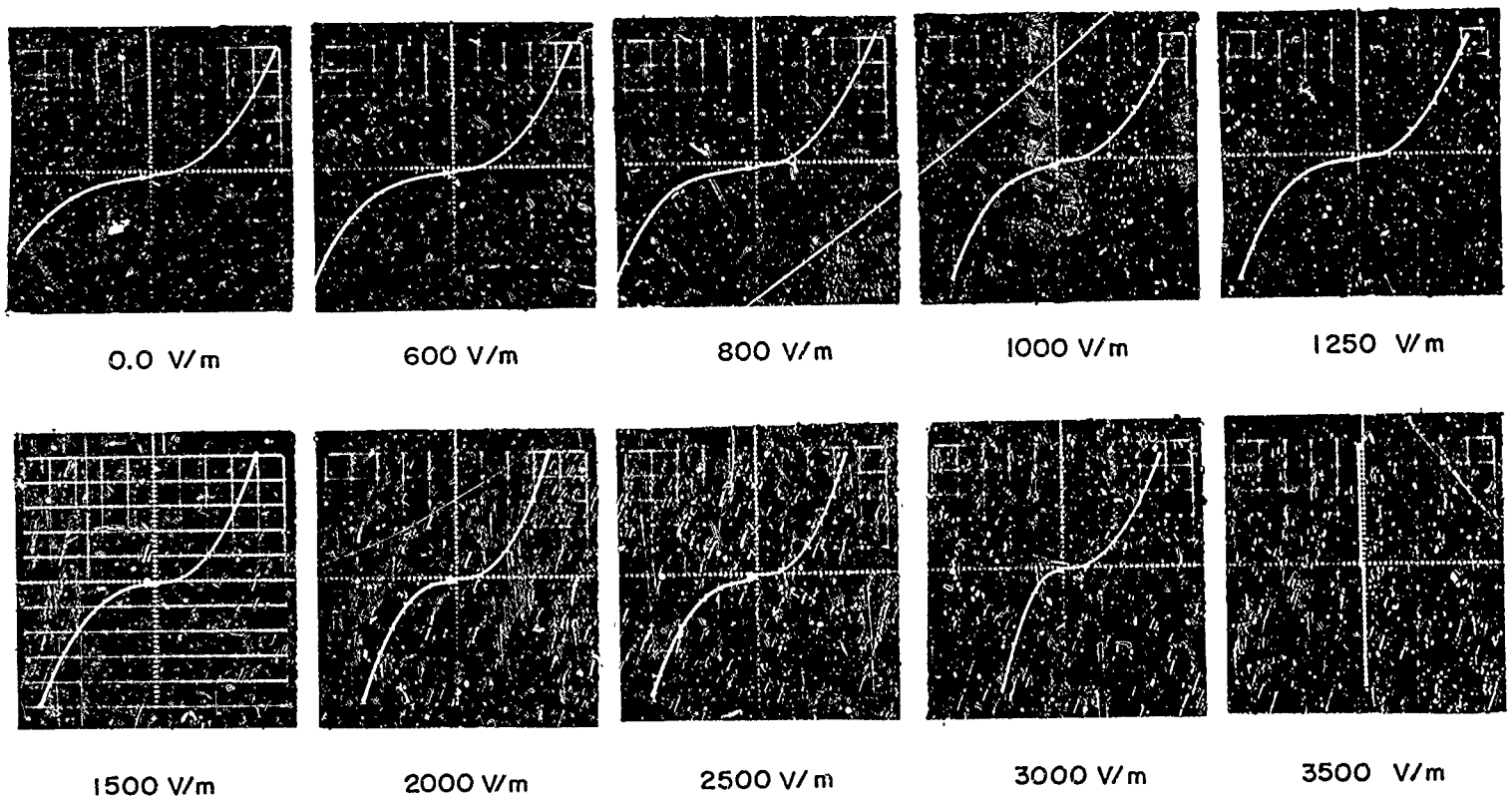

FORWARD AND REVERSE CHARACTERISTICS OBTAINED AFTER EXPOSURE TO FIELD INTENSITIES OF INDICATED VALUES. VERTICAL SCALE FOR THE FORWARD CHARACTERISTICS: 1.0 mA/DIV; FOR THE REVERSE CHARACTERISTICS: 0.02 mA/DIV. HORIZONTAL SCALE FOR THE FORWARD CHARACTERISTICS: 0.2 V/DIV; FOR THE REVERSE CHARACTERISTCS: 20 V/DIV

Figure 13. Electrical characteristics of 1N67-A germanium diode after exposure to EMR—cooled by convection; thermocouple wires removed.

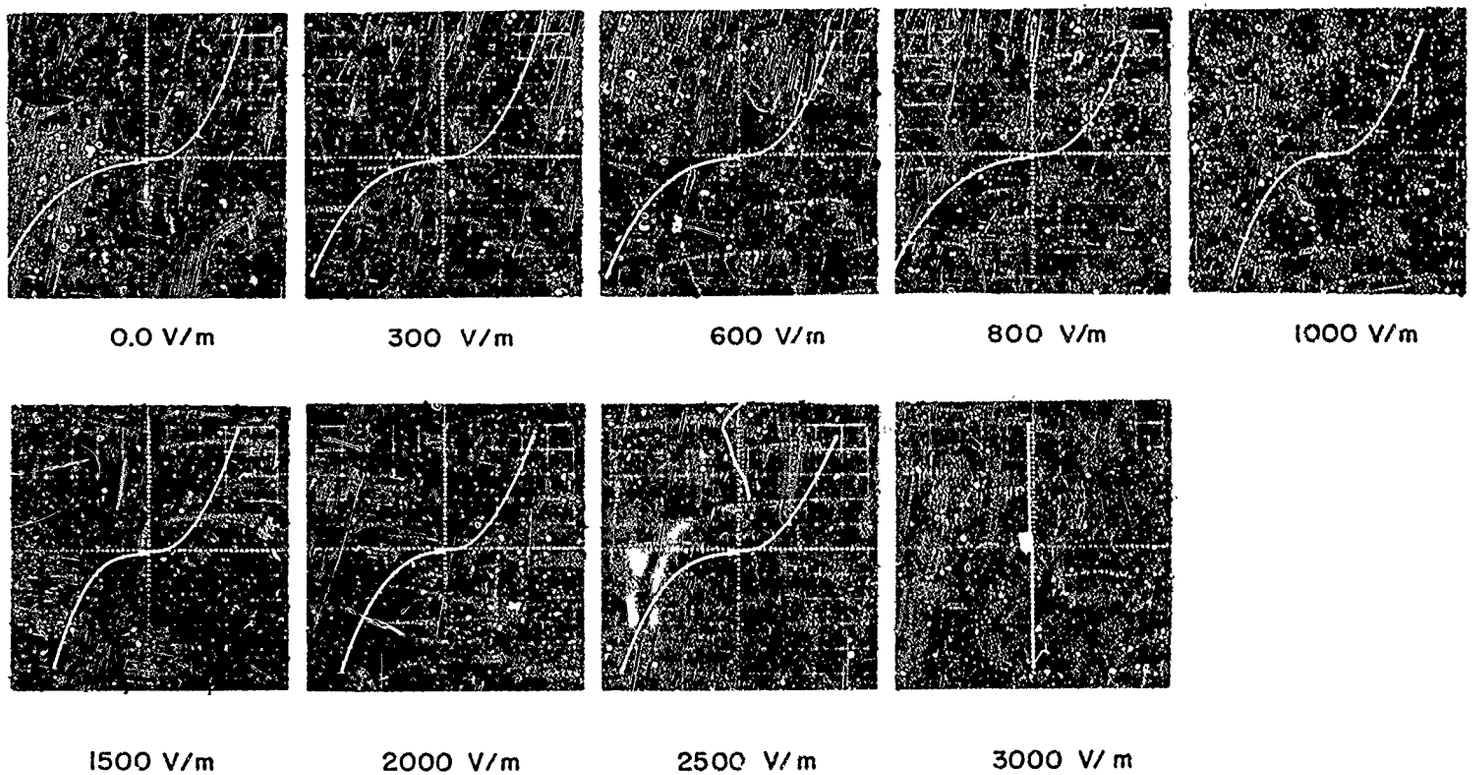

FORWARD AND REVERSE CHARACTERISTICS OBTAINED AFTER EXPOSURE TO FIELD INTENSITIES OF INDICATED VALUES. VERTICAL SCALE FOR THE FORWARD CHARACTERISTICS: 1.0 mA/DIV FOR THE REVERSE CHARACTERISTICS: 0.02 mA/DIV. HORIZONTAL SCALE FOR THE FORWARD CHARACTERISTICS: 0.2 V/DIV; FOR THE REVERSE CHARACTERISTCS 20 V/DIV

Figure 14. Electrical characteristics of 1N67-A germanium diode after exposure to EMR—cooled by convection; thermocouple wires removed.

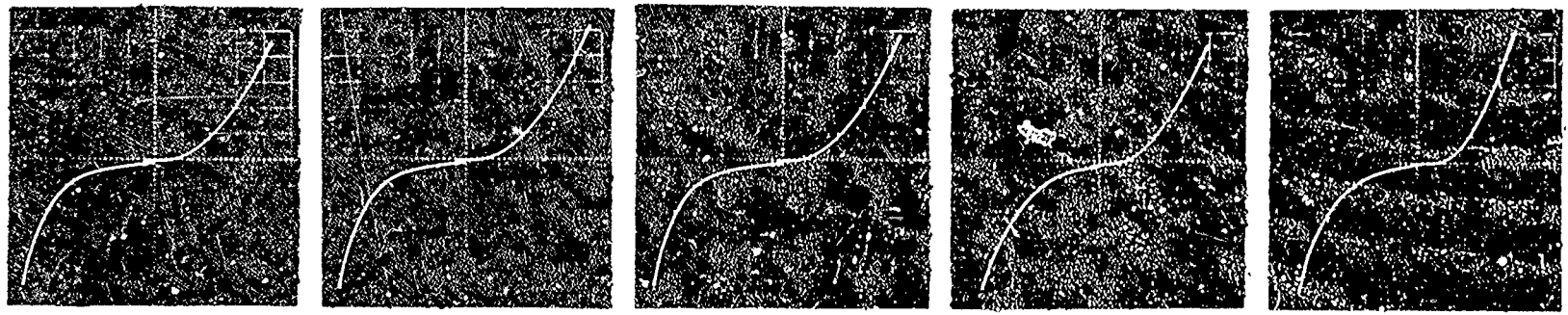

0.0 V/m 800 V/m 1000 V/m 1500 V/m 2000 V/m

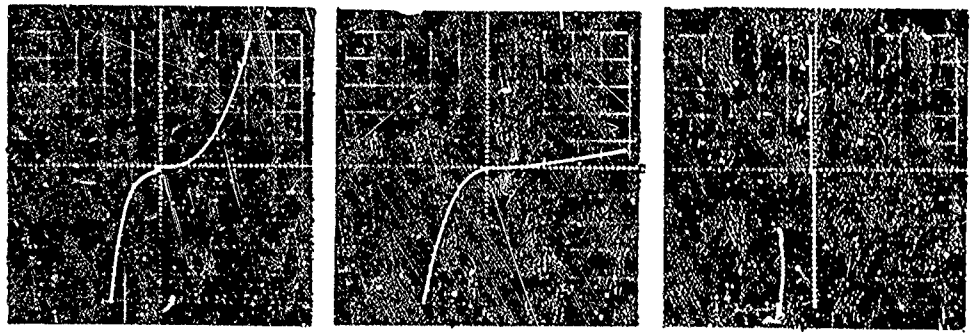

2500 V/m 3000 V/m 3500 V/m

FORWARD AND REVERSE CHARACTERISTICS OBTAINED AFTER EXPOSURE TO FIELD INTENSITIES OF INDICATED VALUES. VERTICAL SCALE FOR THE FORWARD CHARACTERISTICS: 1.0 mA/DIV; FOR THE REVERSE CHARACTERISTICS: 0.02 mA/DIV. HORIZONTAL SCALE FOR THE FORWARD CHARACTERISTICS: 0.2 V/DIV; FOR THE REVERSE CHARACTERISTCS: 20 V/DIV.

Figure 15. Electrical characteristics of 1N67-A germanium diode after exposure to EMR—cooled by convection; thermocouple wires removed.

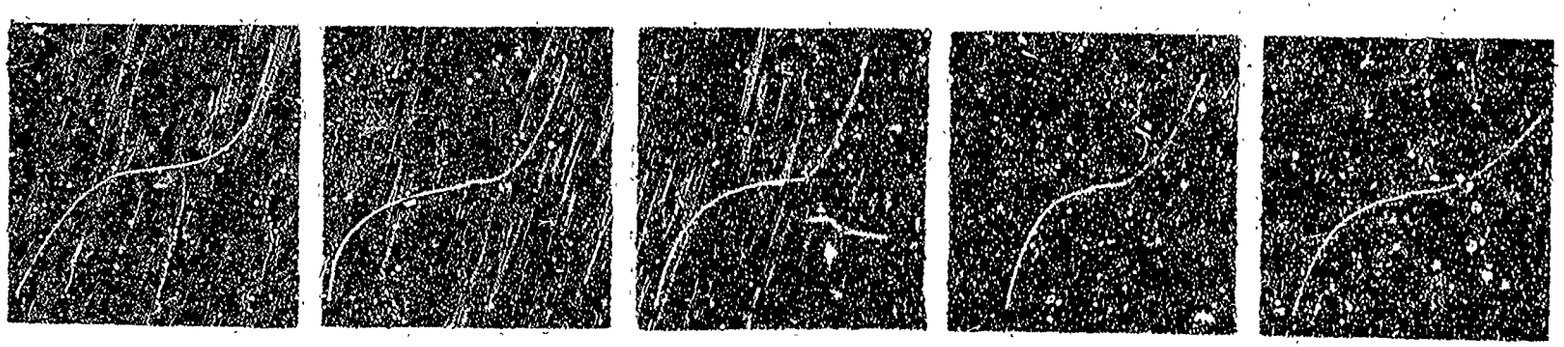

0.0 V/m 800 V/m 1000 V/m 1250 V/m 1500 V/m

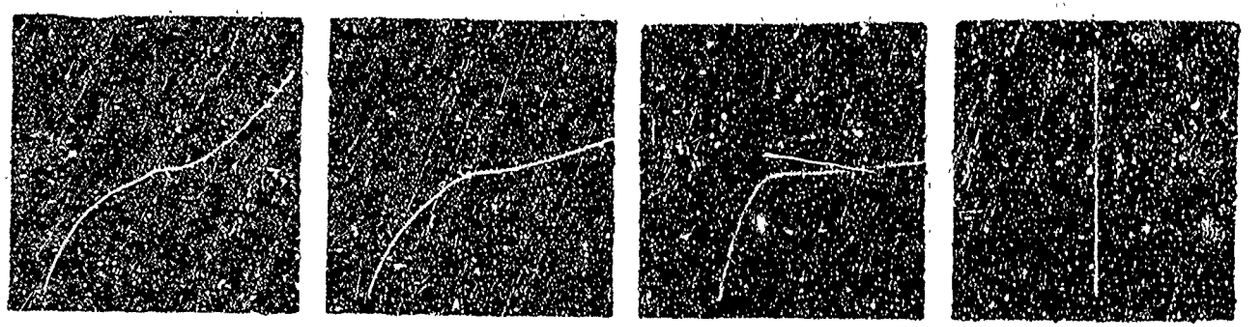

2000 V/m 2500 V/m 3000 V/m 3500 V/m

FORWARD AND REVERSE CHARACTERISTICS OBTAINED AFTER EXPOSURE TO FIELD INTENSITIES OF INDICATED VALUES VERTICAL SCALE FOR THE FORWARD CHARACTERISTICS: 1.0 mA/DIV; FOR THE REVERSE CHARACTERISTICS: 0.02 mA/DIV. HORIZONTAL SCALE FOR THE FORWARD CHARACTERISTICS: 0.2 V/DIV FOR THE REVERSE CHARACTERISTCS: 20 V/DIV

Figure 16. Electrical characteristics of 1N67-A germanium diode after exposure to EMR—cooled by convection; thermocouple wires removed.

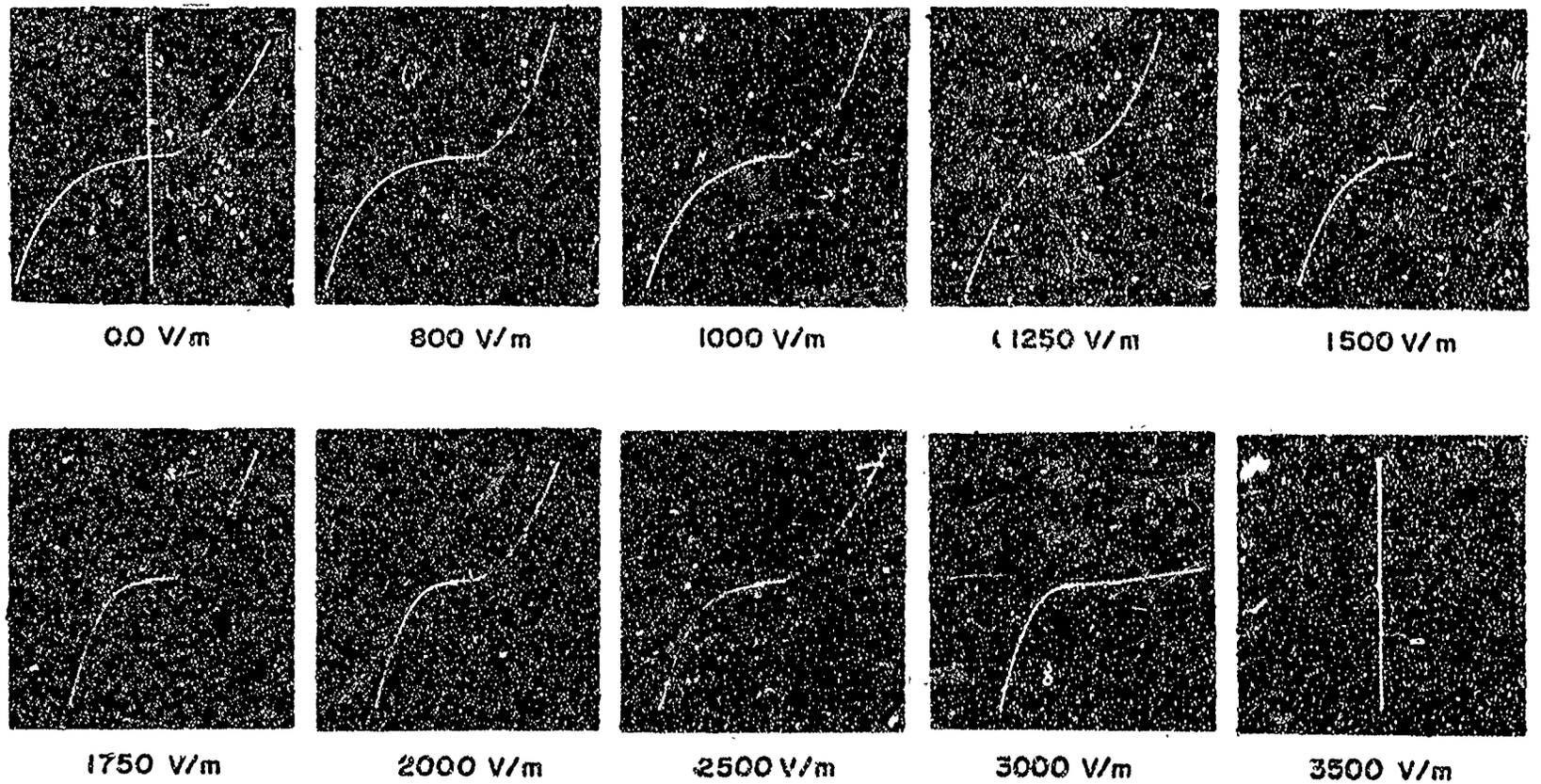

FORWARD AND REVERSE CHARACTERISTICS OBTAINED AFTER EXPOSURE TO FIELD INTENSITIES OF INDICATED VALUES. VERTICAL SCALE FOR THE FORWARD CHARACTERISTICS: 1.0 mA/DIV; FOR THE REVERSE CHARACTERISTICS: 0.02 mA/DIV. HORIZONTAL SCALE FOR THE FORWARD CHARACTERISTICS: 0.2 V/DIV; FOR THE REVERSE CHARACTERISTCS: 20 V/DIV.

Figure 17. Electrical characteristics of 1N67-A germanium diode after exposure to EMR—cooled by convection; thermocouple wires removed.

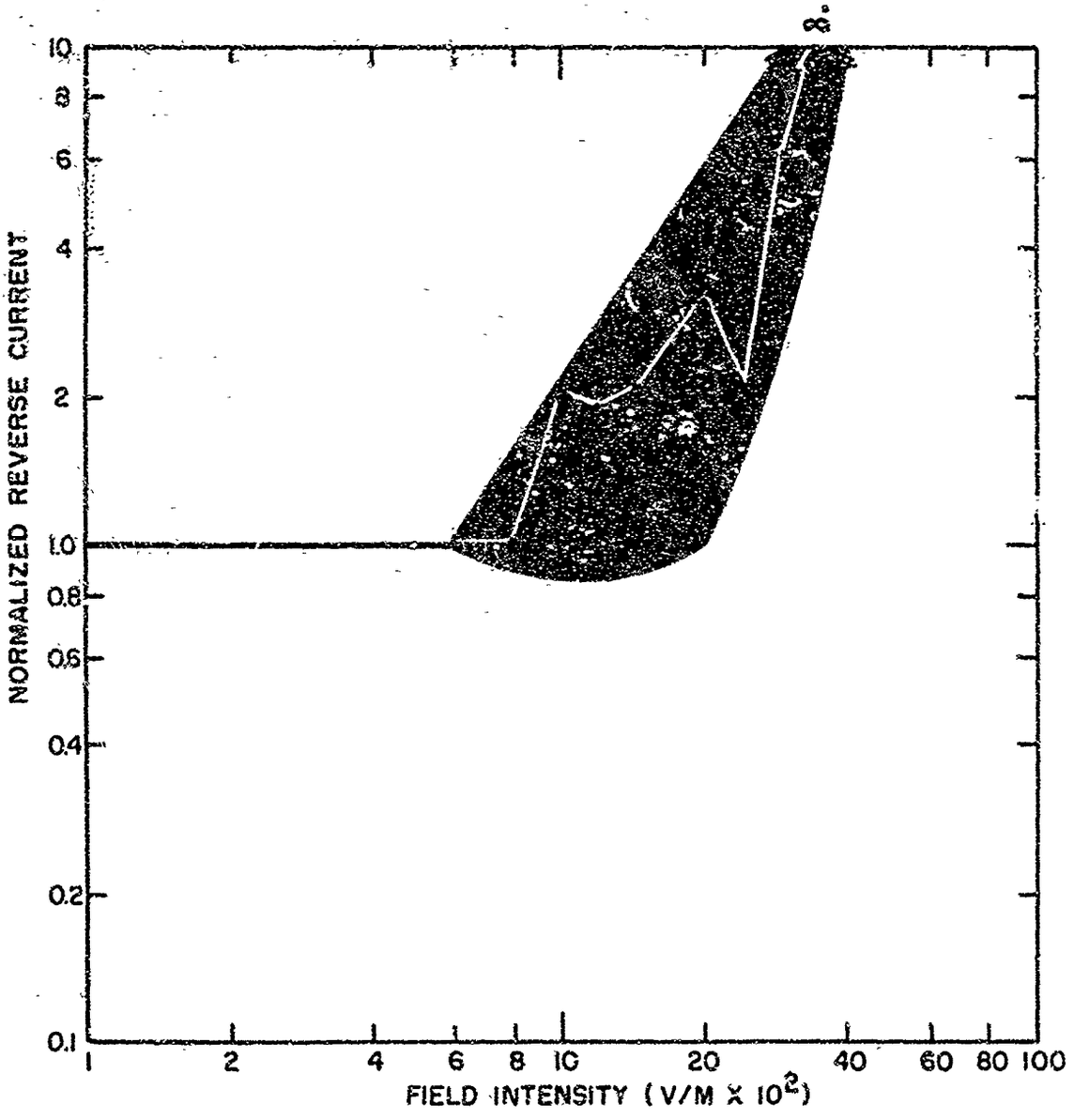

Figure 18. Normalized reverse current of 1N67-A germanium diode after exposure to EMR; reverse characteristics at V_r=60 V.

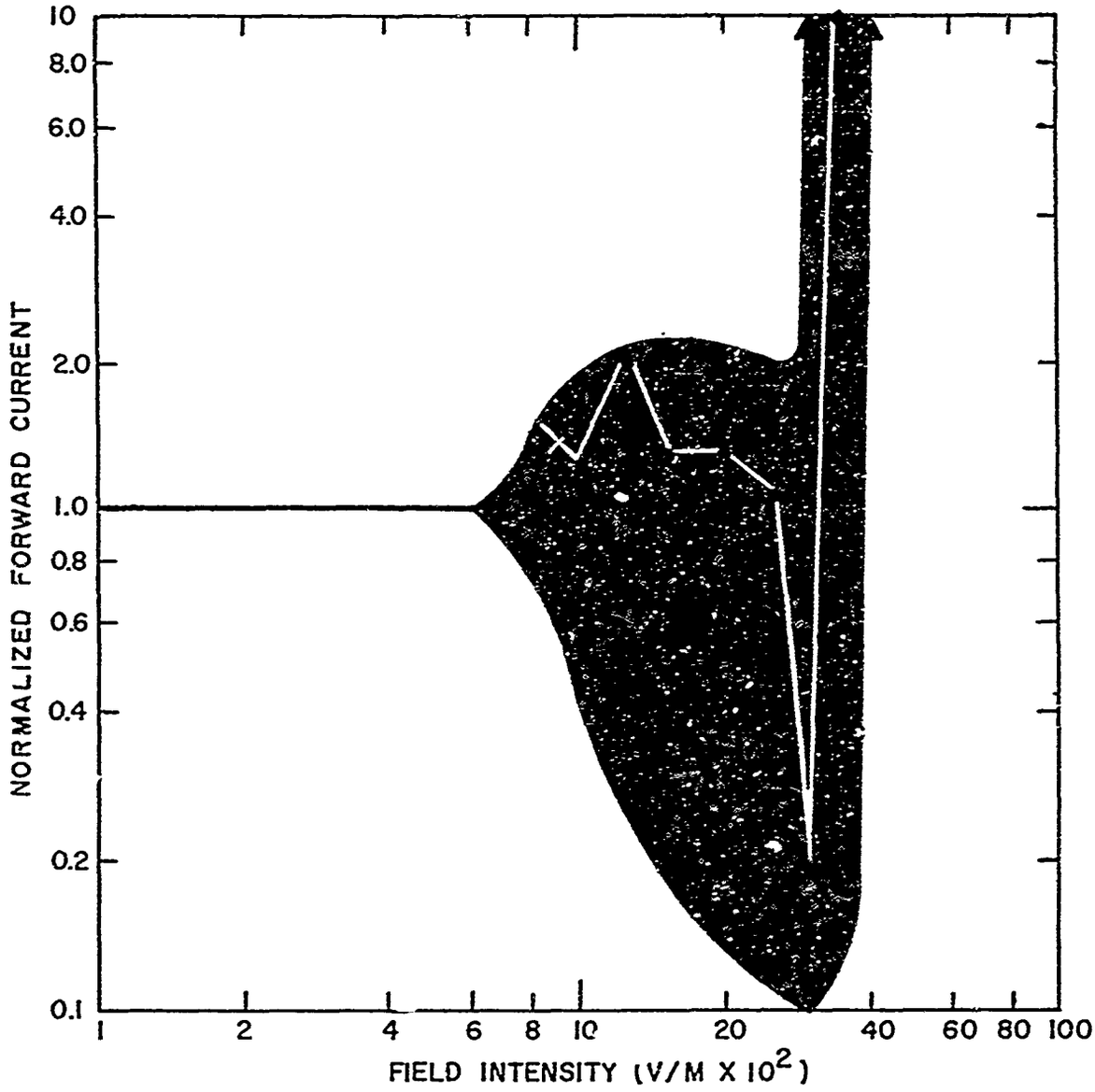

Figure 19. Normalized forward current of 1N67-A germanium diode after exposure to EMR; forward current at 0.6-V curve for typical diode and spread for 90 percent of measured samples.

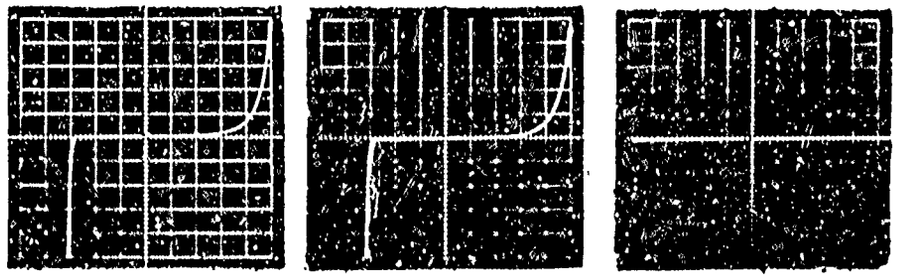

0.0 V/m 3000 V/m 3500 V/m

FORWARD AND REVERSE CHARACTERISTICS OBTAINED AFTER EXPOSURE TO FIELD INTENSITIES OF INDICATED VALUES. VERTICAL SCALE FOR THE FORWARD CHARACTERISTICS: 0.02 mA/DIV; FOR THE REVERSE CHARACTERISTICS; 0.02 mA/DIV. HORIZONTAL SCALE FOR THE FORWARD CHARACTERISTICS: 0.1 V/DIV; FOR THE REVERSE CHARACTERISTICS; 50 V/DIV.

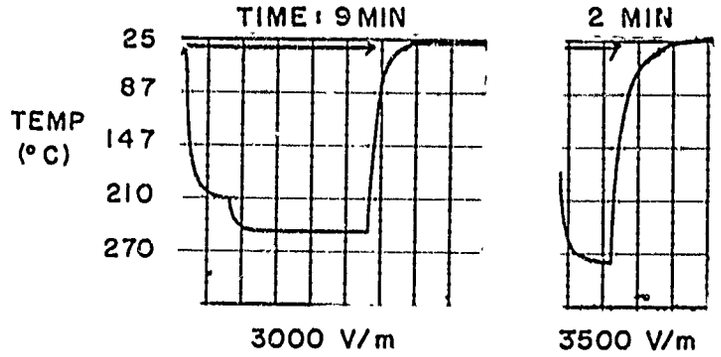

TEMPERATURE OF THE DIODE MEASURED AT THE CATHODE LEAD AS THE DIODE WAS EXPOSED TO rf RADIATION OF INDICATED FIELD INTENSITIES

Figure 20. Electrical characteristics of 1N3066 silicon diode after exposure to EMR—cooled by convection.

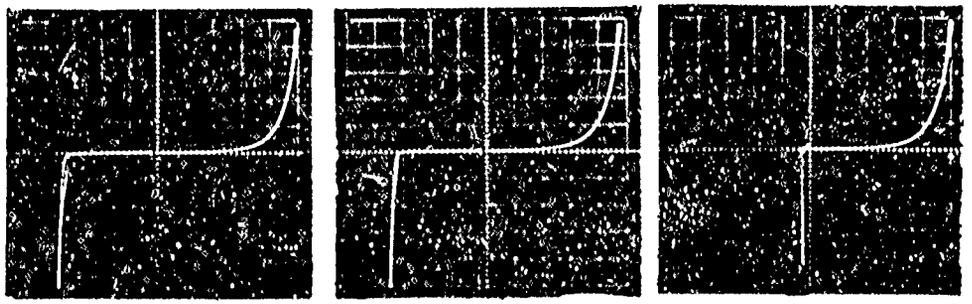

0.0 V/m 3500 V/m 4000 V/m

FORWARD AND REVERSE CHARACTERISTICS OBTAINED AFTER EXPOSURE TO FIELD INTENSITIES OF INDICATED VALUES. VERTICAL SCALE FOR THE FORWARD CHARACTERISTICS: 0.02 mA/DIV; FOR THE REVERSE CHARACTERISTICS; 0.02 mA/DIV. HORIZONTAL SCALE FOR THE FORWARD CHARACTERISTICS: 0.1 V/DIV; FOR THE REVERSE CHARACTERISTICS; 50 V/DIV.

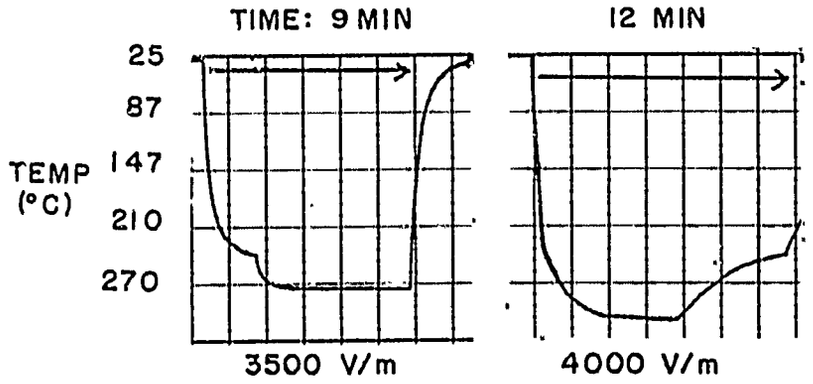

TEMPERATURE OF THE DIODE MEASURED AT THE CATHODE LEAD AS THE DIODE WAS EXPOSED TO rf RADIATION OF INDICATED FIELD INTENSITIES.

Figure 21. Electrical characteristics of 1N3066 silicon diode after exposure to EMR—cooled by convection.

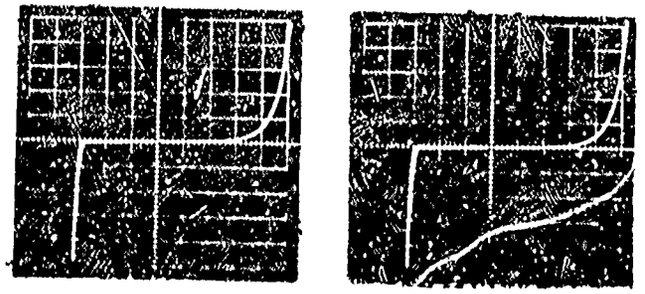

0.0 V/m 4000 V/m

FORWARD AND REVERSE CHARACTERISTICS OBTAINED AFTER EXPOSURE TO FIELD INTENSITIES OF INDICATED VALUES. VERTICAL SCALE FOR THE FORWARD CHARACTERISTICS: 0.02 mA/DIV; FOR THE REVERSE CHARACTERISTICS; 0.02 mA/DIV. HORIZONTAL SCALE FOR THE FORWARD CHARACTERISTICS: 0.1 V/DIV; FOR THE REVERSE CHARACTERISTICS; 50 V/DIV.

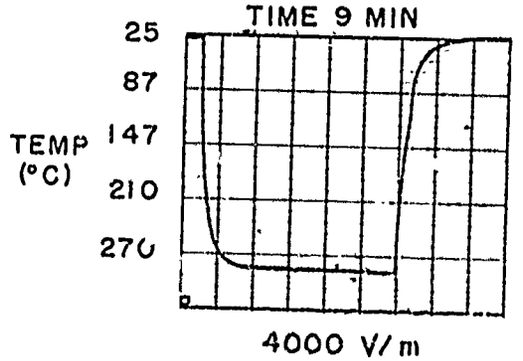

TEMPERATURE OF THE DIODE MEASURED AT THE CATHODE LEAD AS THE DIODE WAS EXPOSED TO rf RADIATION OF INDICATED FIELD INTENSITIES.

Figure 22. Electrical characteristics of 1N3066 silicon diode after exposure to EMR--cooled by convection.

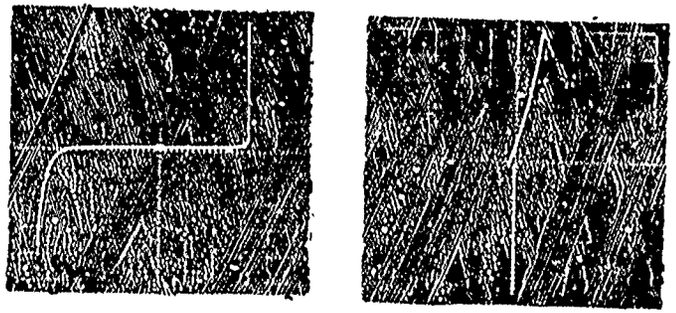

0.0 V/m 2000 V/m

FORWARD AND REVERSE CHARACTERISTICS OBTAINED AFTER EXPOSURE TO FIELD INTENSITIES OF INDICATED VALUES. VERTICAL SCALE FOR THE FORWARD CHARACTERISTICS: 0.02 mA/DIV; FOR THE REVERSE CHARACTERISTICS; 0.02 mA/DIV. HORIZONTAL SCALE FOR THE FORWARD CHARACTERISTICS: 0.1 V/DIV; FOR THE REVERSE CHARACTERISTICS; 10.0V/DIV.

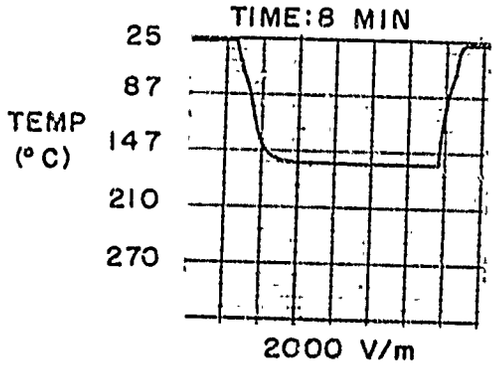

TEMPERATURE OF THE DIODE MEASURED AT THE CATHODE LEAD AS THE DIODE WAS EXPOSED TO rf RADIATION OF INDICATED FIELD INTENSITIES.

Figure 23. Electrical characteristics of HP-2201 silicon diode after exposure to EMR—cooled by convection.

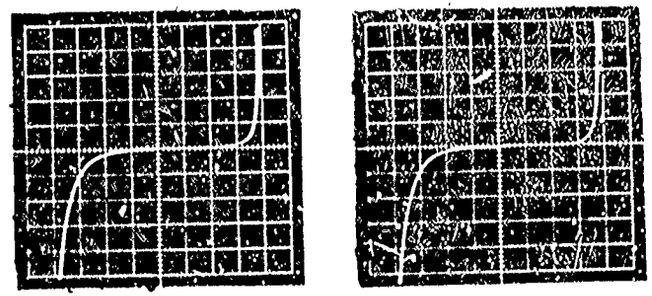

0.0 V/m 4000 V/m

FORWARD AND REVERSE CHARACTERISTICS OBTAINED AFTER EXPOSURE TO FIELD INTENSITIES OF INDICATED VALUES VERTICAL SCALE FOR THE FORWARD CHARACTERISTICS: 10 mA/DIV; FOR THE REVERSE CHARACTERISTICS: 0.5 mA/DIV HORIZONTAL SCALE FOR THE FORWARD CHARACTERISTICS: 0.2 V/DIV: FOR THE REVERSE CHARACTERISTICS: 0.5 V/DIV

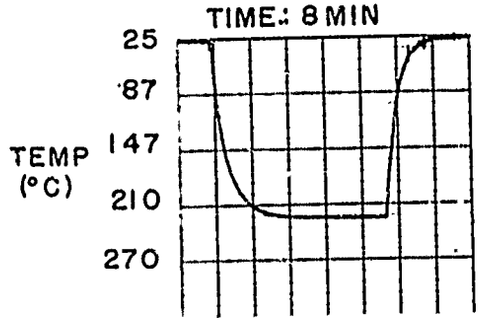

TEMPERATURE OF THE DIODE MEASURED AT THE CATHODE LEAD AS THE DIODE WAS EXPOSED TO rf RADIATION OF INDICATED FIELD INTENSITIES.

Figure 24. Electrical characteristics of 1N747-A silicon reference diode with exposure to EMR—cooled by convection.

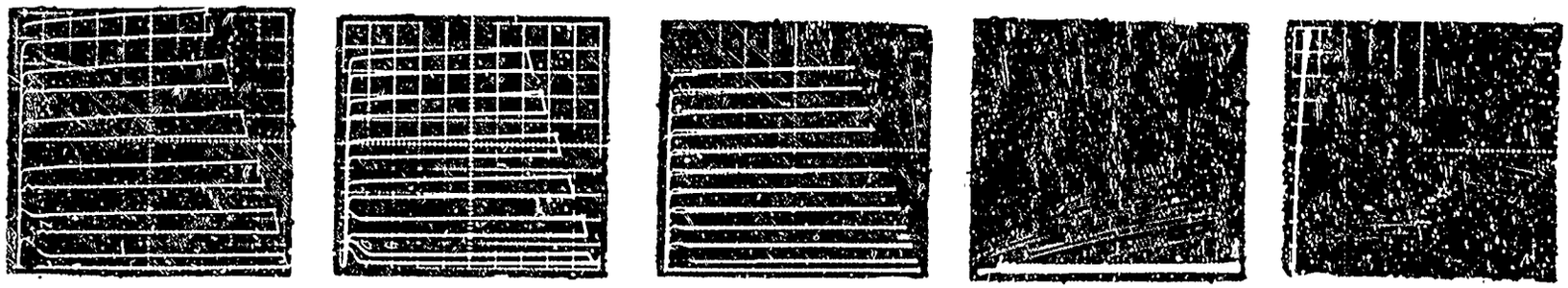

COLLECTOR CHARACTERISTICS OBTAINED AFTER EXPOSURE TO FIELD INTENSITIES OF INDICATED VALUES VERTICAL SCALE 0.1 mA/DIV; HORIZONTAL SCALE 1.0 V/DIV; 0.001 mA/STEP

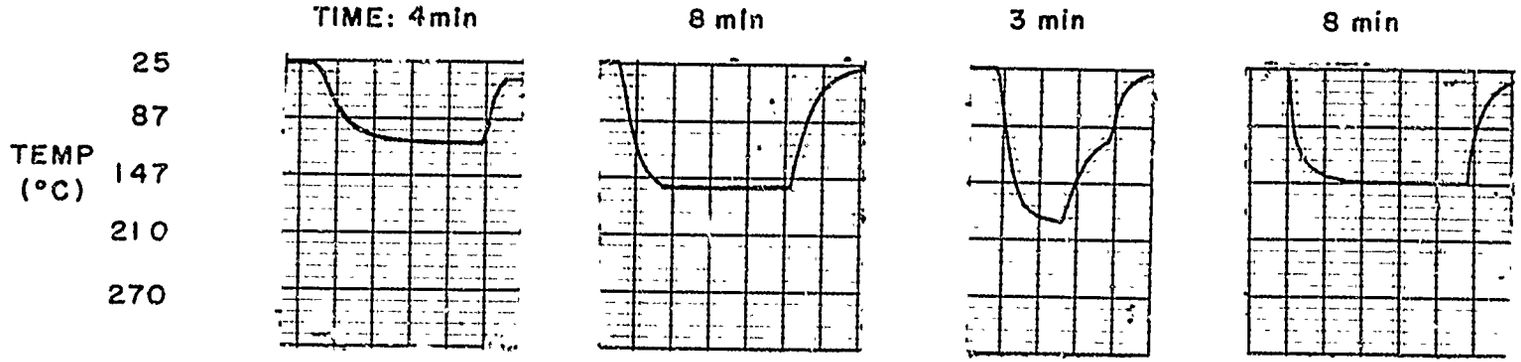

TEMPERATURE OF THE TRANSISTOR MEASURED AT THE COLLECTOR AS THE TRANSISTOR WAS EXPOSED TO rf RADIATION OF INDICATED FIELD INTENSITIES

Figure 25. Electrical characteristics of 2N2714 silicon transistor after exposure to EMR—cooled by convection.

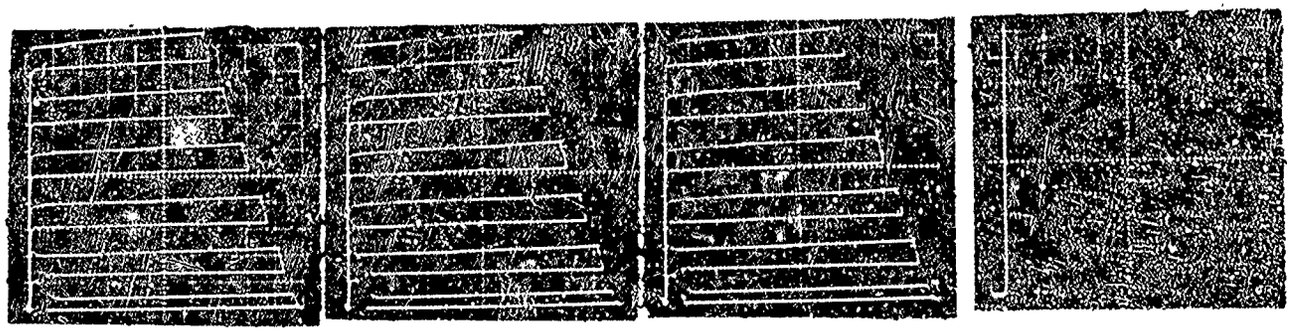

0.0 V/m 800 V/m 1000 V/m 1200 V/m

COLLECTOR CHARACTERISTICS OBTAINED AFTER EXPOSURE TO FIELD INTENSITIES OF INDICATED VALUES. VERTICAL SCALE 0.1 mA/DIV; HORIZONTAL SCALE 1.0 V/DIV; 0.001 mA/STEP

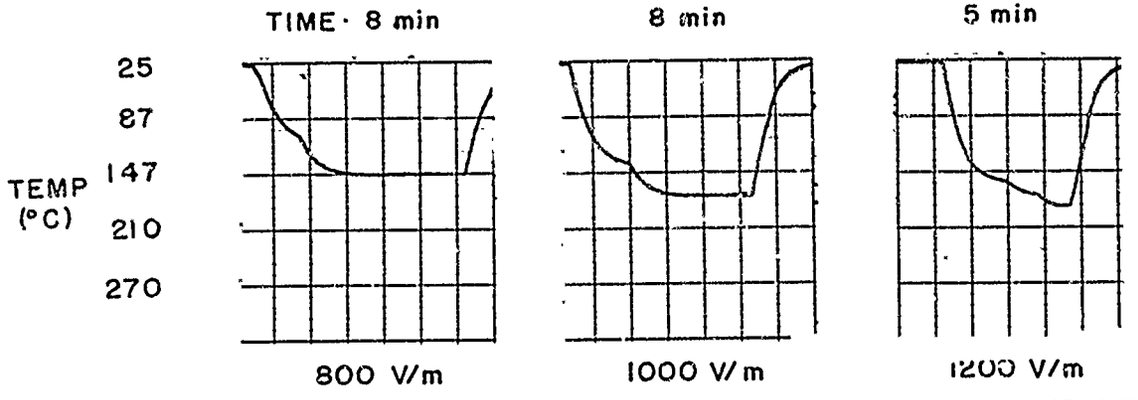

TEMPERATURE OF THE TRANSISTOR MEASURED AT THE COLLECTOR AS THE TRANSISTOR WAS EXPOSED TO rf RADIATION OF INDICATED FIELD INTENSITIES

Figure 26. Electrical characteristics of 2N2714 silicon transistor after exposure to EMR—cooled by convection.

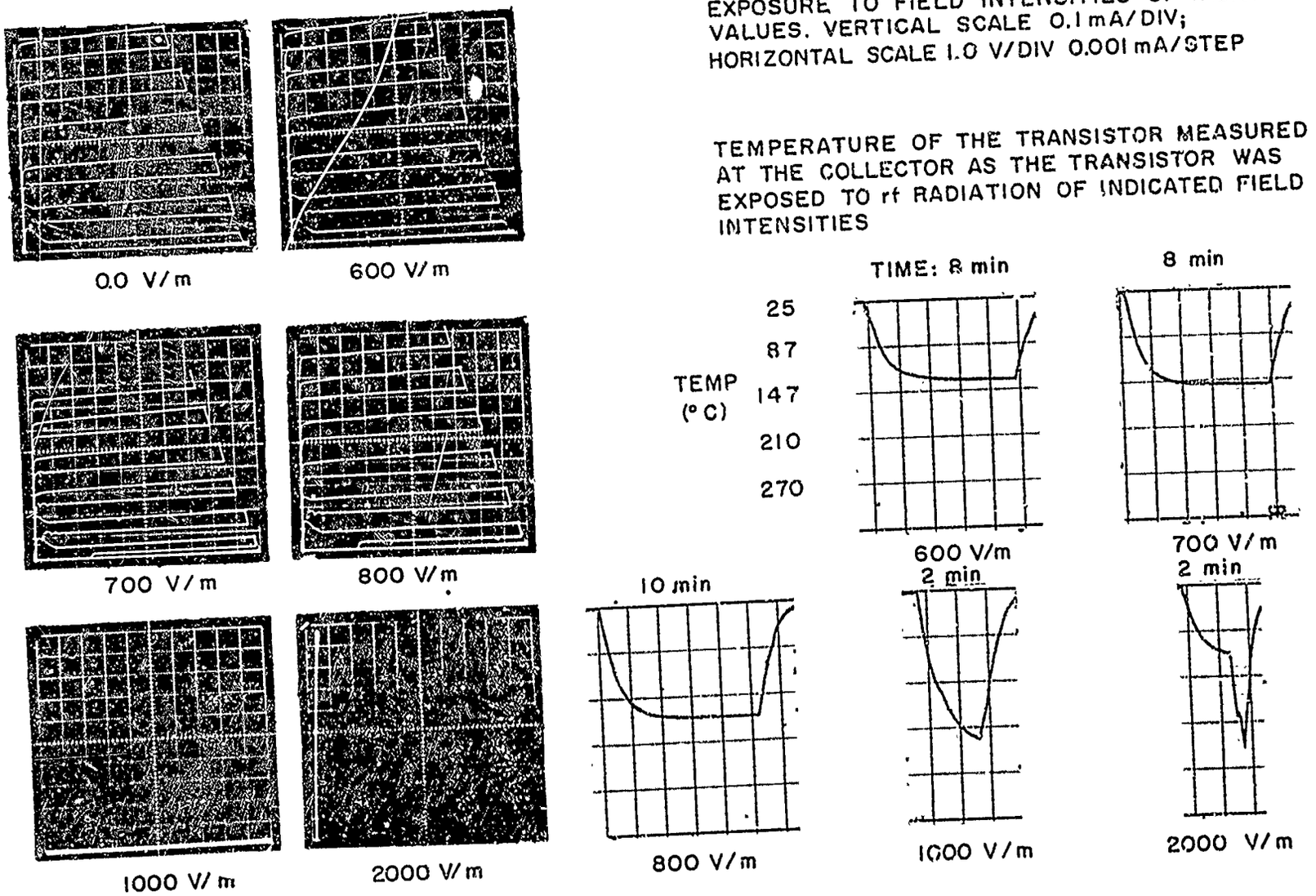

Figure 27. Electrical characteristics of 2N2714 silicon transistor after exposure to EMR—cooled by convection.

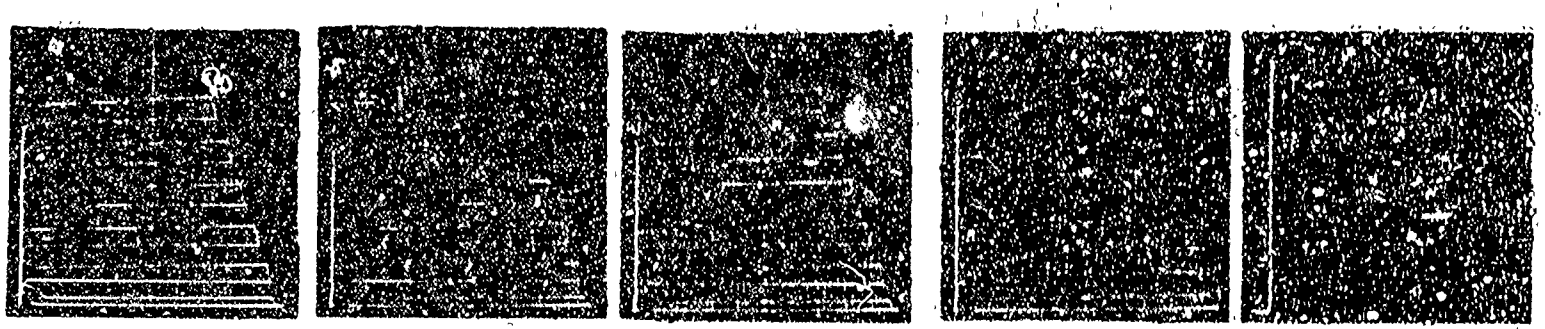

COLLECTOR CHARACTERISTICS OBTAINED AFTER EXPOSURE TO FIELD INTENSITIES OF INDICATED VALUES. VERTICAL SCALE 0.1 mA/DIV; HORIZONTAL SCALE 1.0 V/DIV; 0.001 mA/STEP

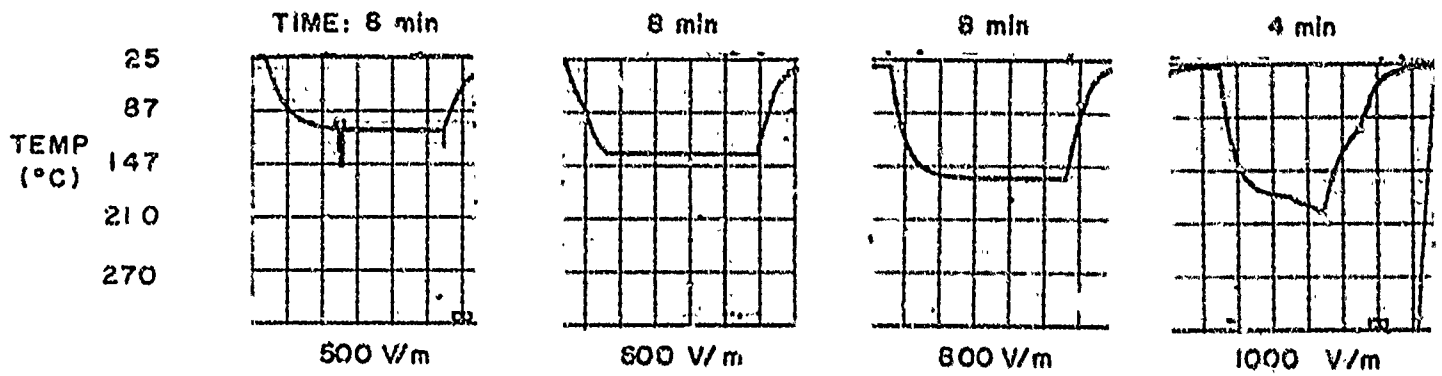

TEMPERATURE OF THE TRANSISTOR MEASURED AT THE COLLECTOR AS THE TRANSISTOR WAS EXPOSED TO rf RADIATION OF INDICATED FIELD INTENSITIES

Figure 28a. Electrical characteristics of 2N2714 silicon transistor after exposure to EMR—cooled by convection.

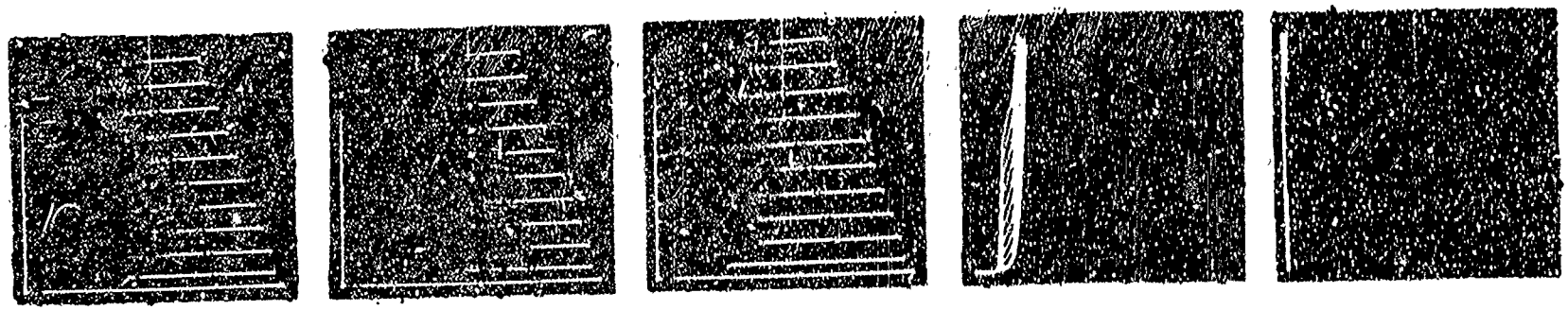

COLLECTOR CHARACTERISTICS OBTAINED AFTER EXPOSURE TO FIELD INTENSITIES OF INDICATED VALUES. VERTICAL SCALE 0.1 mA/DIV; HORIZONTAL SCALE 1.0 V/DIV; 0.001 mA/STEP

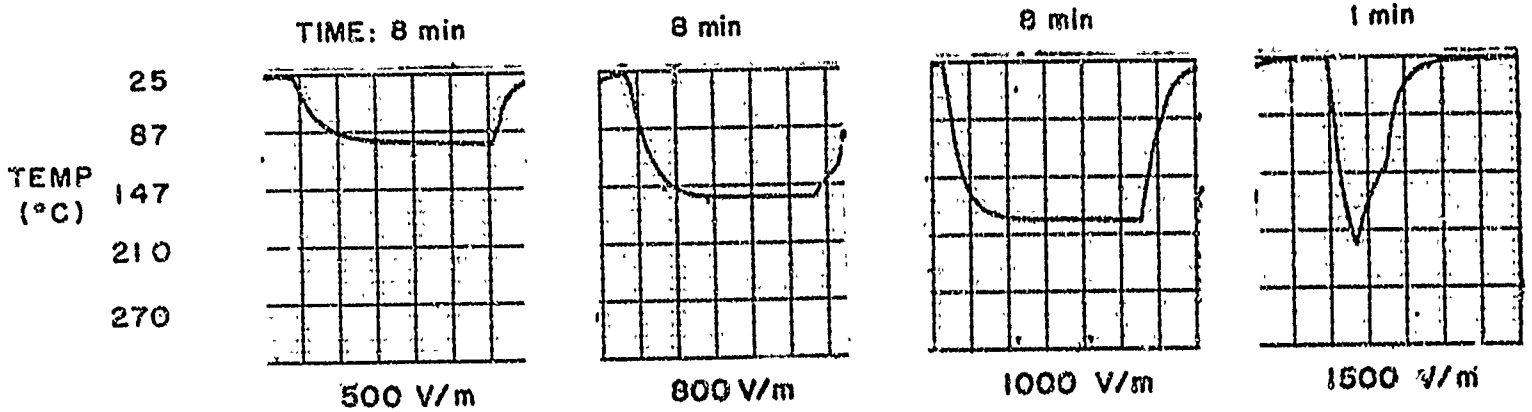

TEMPERATURE OF THE TRANSISTOR MEASURED AT THE COLLECTOR AS THE TRANSISTOR WAS EXPOSED TO rf RADIATION OF INDICATED FIELD INTENSITIES.

Figure 28b. Electrical characteristics of 2N2714 silicon transistor after exposure to EMR—cooled by convection.

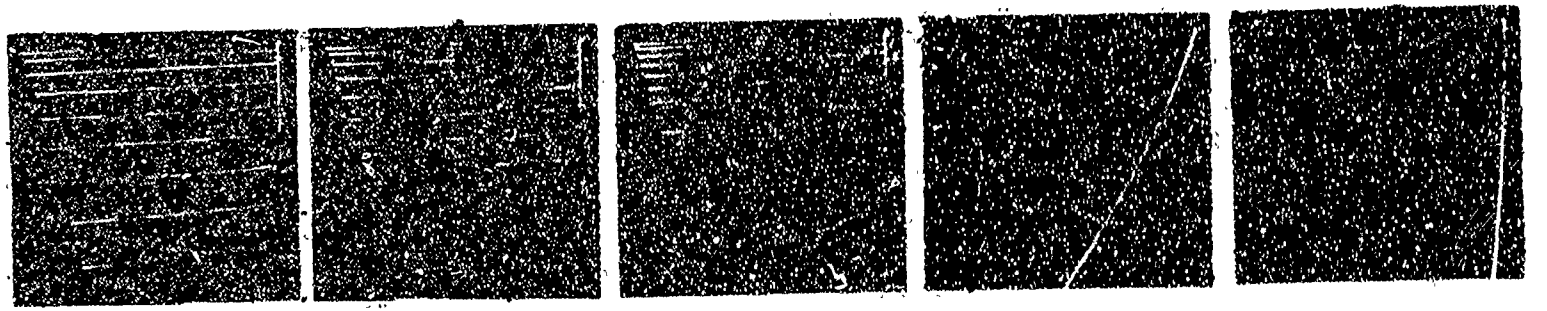

0.0 V/m 600 V/m 700 V/m 800 V/m 1000 V/m

COLLECTOR CHARACTERISTICS OBTAINED AFTER EXPOSURE TO FIELD INTENSITIES OF INDICATED VALUES. VERTICAL SCALE 0.02 mA/DIV; HORIZONTAL SCALE 0.5 V/DIV; 0.002 mA/STEP

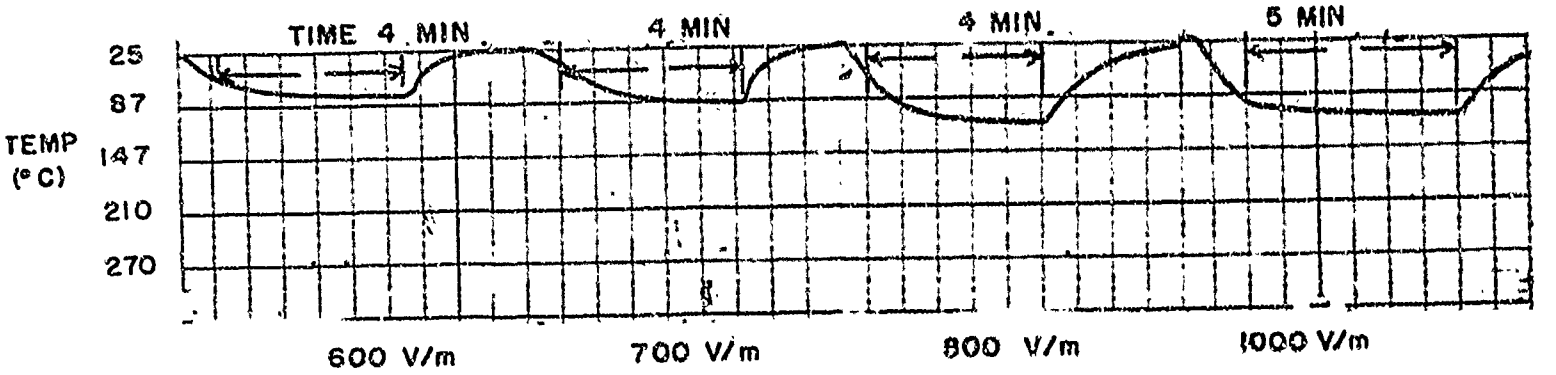

TEMPERATURE OF THE TRANSISTOR MEASURED AT THE COLLECTOR AS THE TRANSISTOR WAS EXPOSED TO rf RADIATION OF INDICATED FIELD INTENSITIES.

Figure 29. Electrical characteristics of 2N3785 germanium transistor after exposure to EMR—cooled by convection.

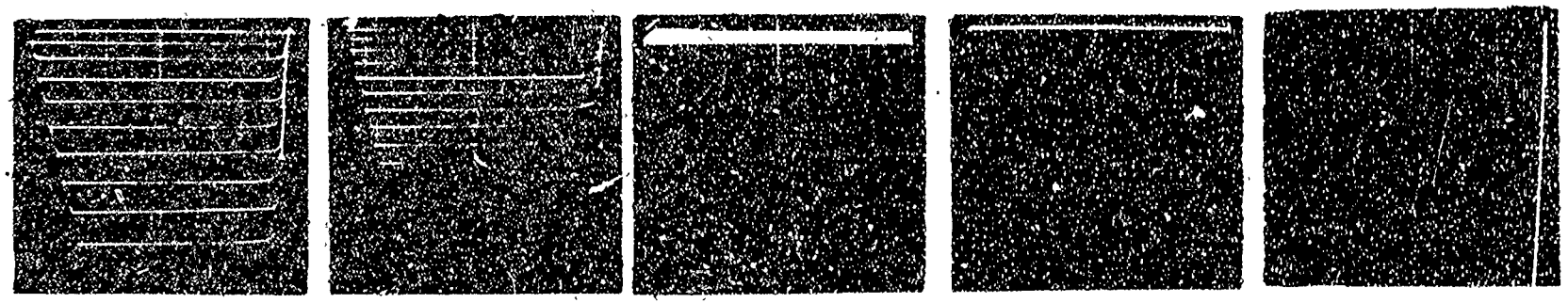

0.0 V/m 600 V/m 700 V/m 800 V/m 1000 V/m

COLLECTOR CHARACTERISTICS OBTAINED AFTER EXPOSURE TO FIELD INTENSITIES OF INDICATED VALUES. VERTICAL SCALE 0.02 mA/DIV; HORIZONTAL SCALE 0.5 V/DIV; 0.002 mA/STEP

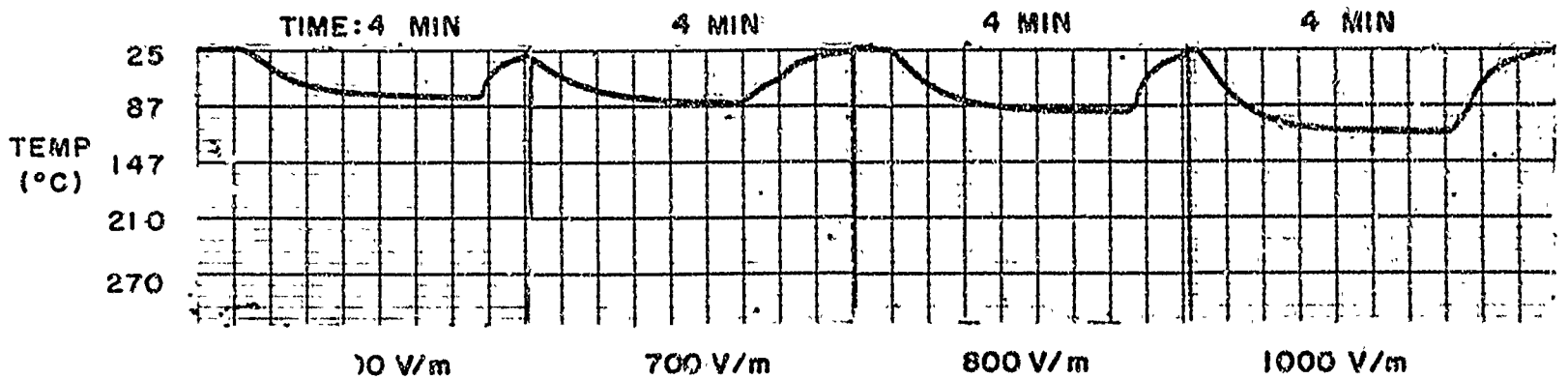

TEMPERATURE OF THE TRANSISTOR MEASURED AT THE COLLECTOR AS THE TRANSISTOR WAS EXPOSED TO rf RADIATION OF INDICATED FIELD INTENSITIES.

Figure 30. Electrical characteristics of 2N3785 germanium transistor after exposure to EMR—cooled by convection.

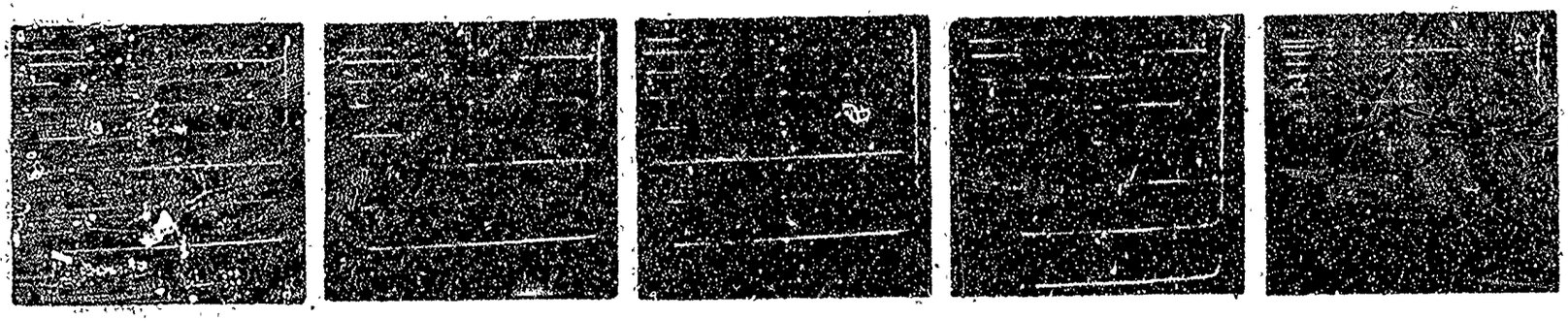

COLLECTOR CHARACTERISTICS OBTAINED AFTER EXPOSURE TO FIELD INTENSITIES OF INDICATED VALUES. VERTICAL SCALE 0.02 mA/DIV; HORIZONTAL SCALE 0.5 V/DIV; 0.002 mA/STEP

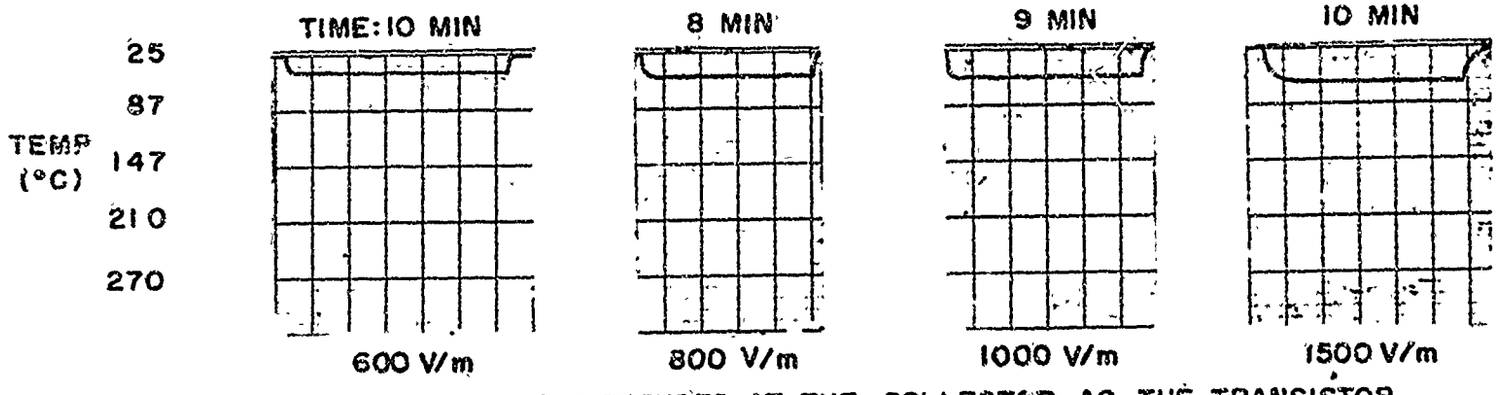

TEMPERATURE OF THE TRANSISTOR MEASURED AT THE COLLECTOR AS THE TRANSISTOR WAS EXPOSED TO rf RADIATION OF INDICATED FIELD INTENSITIES.

Figure 31. Electrical characteristics of 2N3785 germanium transistor after exposure to EMR—cooled by convection.

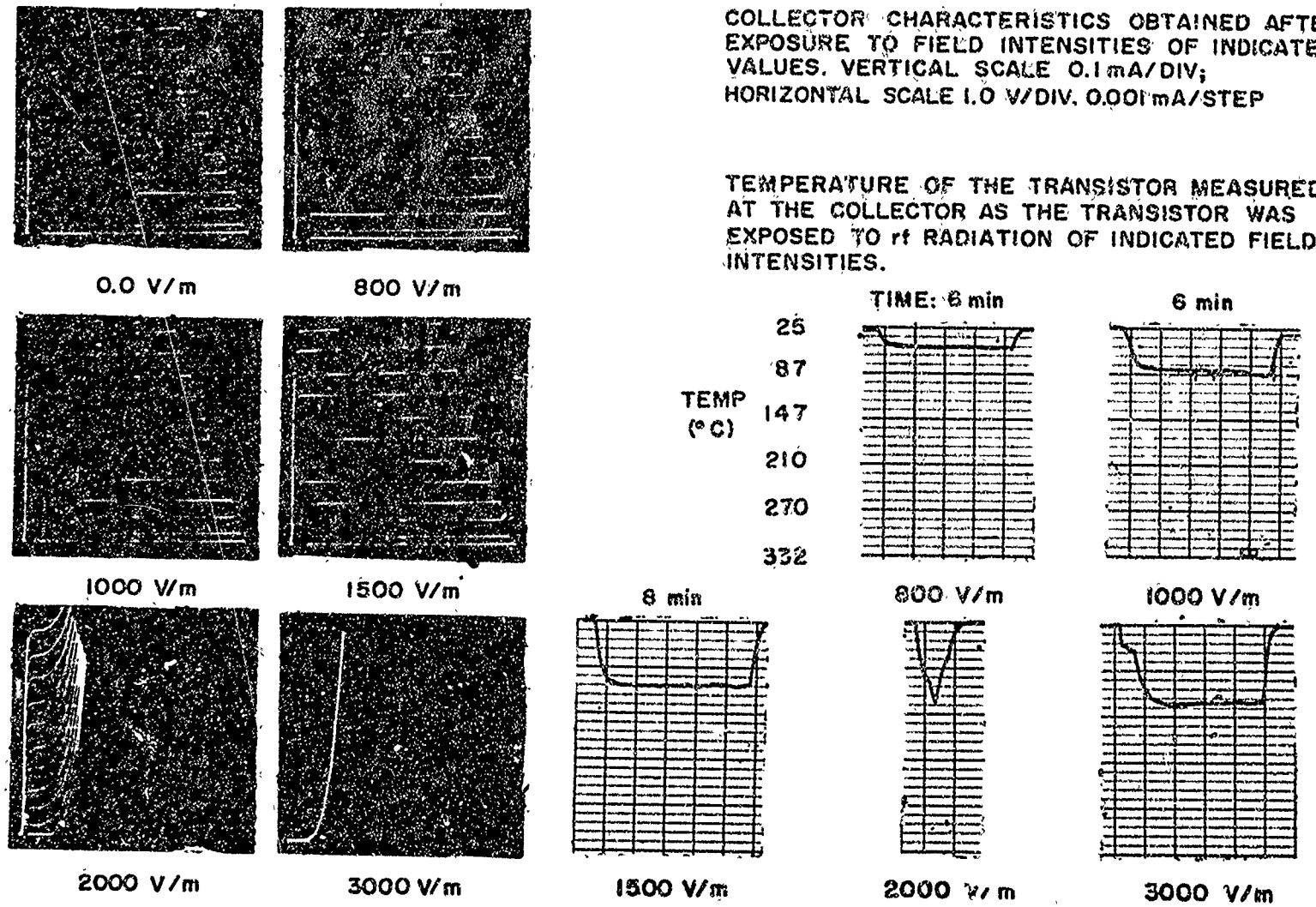

Figure 32. Electrical characteristics of 2N2714 silicon transistor after exposure—forced-air cooled.

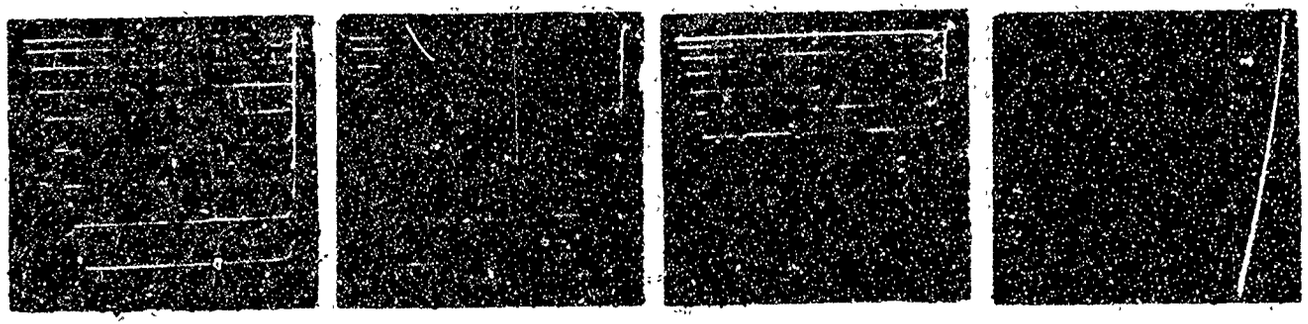

0.0 V/m 500 V/m 600 V/m 800 V/m

COLLECTOR CHARACTERISTICS OBTAINED AFTER EXPOSURE TO FIELD INTENSITIES OF INDICATED VALUES. VERTICAL SCALE 0.02mA/DIV; HORIZONTAL SCALE 0.5V/DIV; 0.002mA/STEP

Figure 33. Electrical characteristics of 2N3785 germanium transistor after exposure to EMR—cooled by convection; thermocouple wires removed.

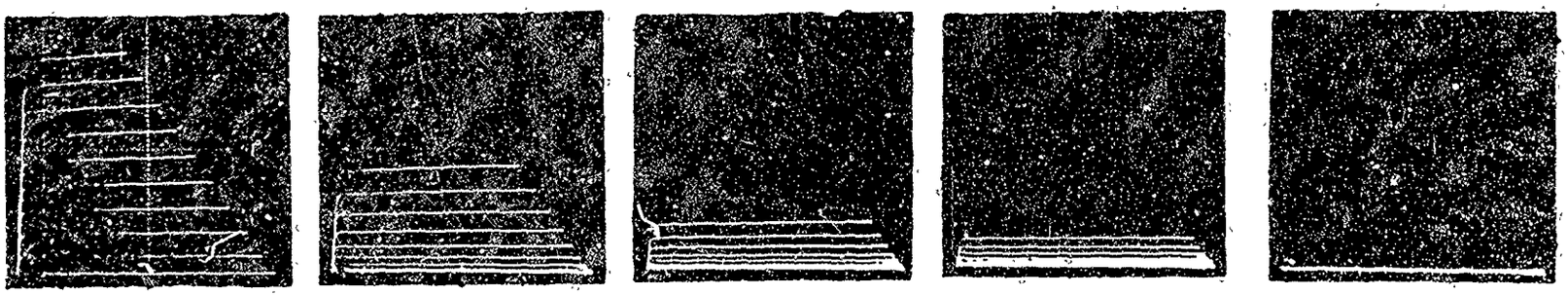

0.0 V/m 800 V/m 1000 V/m 1100 V/m 1500 V/m

COLLECTOR CHARACTERISTICS OBTAINED AFTER EXPOSURE TO FIELD INTENSITIES OF INDICATED VALUES. VERTICAL SCALE 0.1 mA/DIV; HORIZONTAL SCALE 1.0 V/DIV; 0.001 mA/STEP

Figure 34. Electrical characteristics of 2N2714 silicon transistor after exposure to EMR—cooled by convection; thermocouple wires removed.

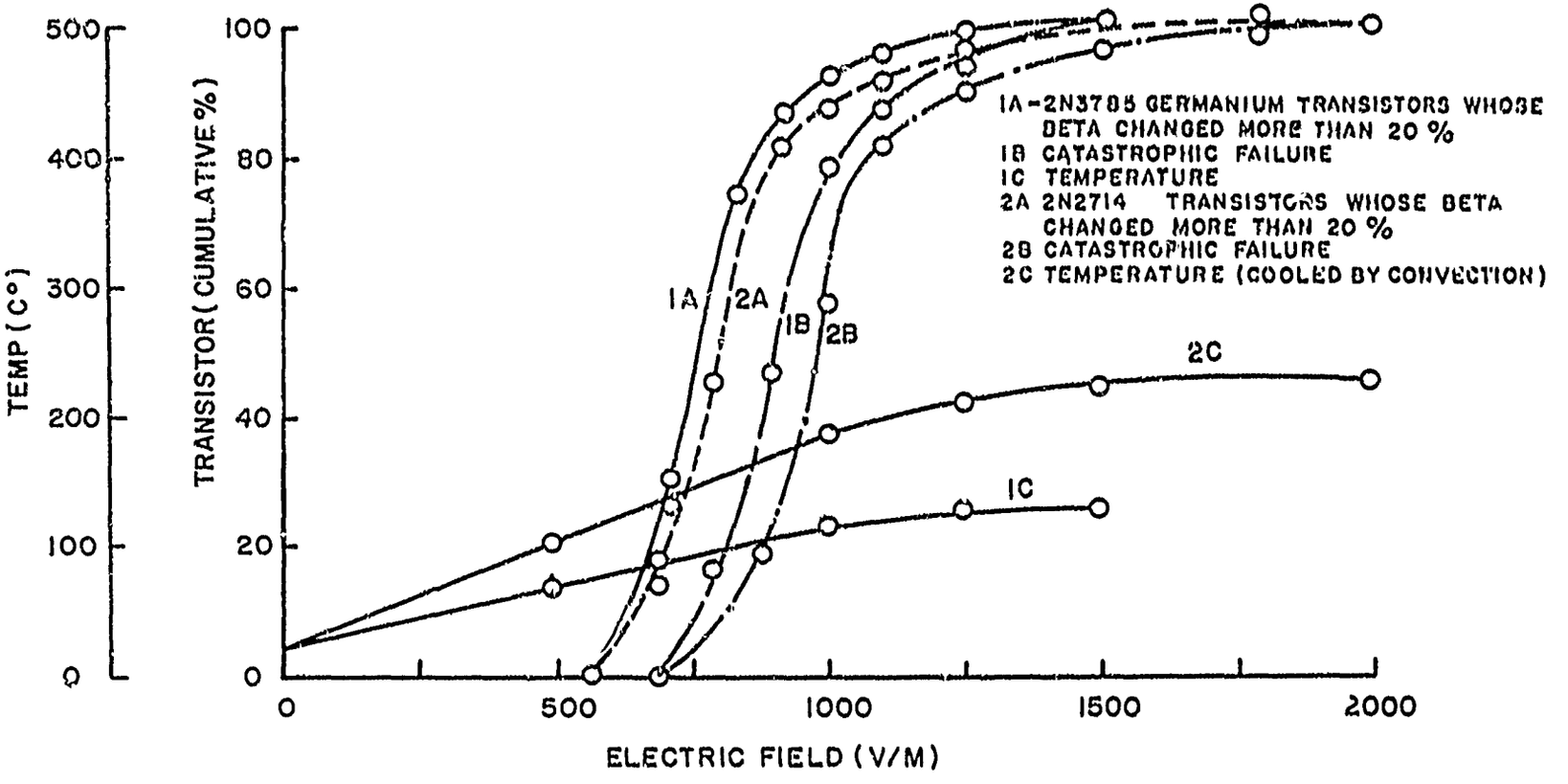

Figure 35. Cumulative distribution of transistors experiencing changes in electrical characteristics versus electric field.

DRAIN CHARACTERISTICS OBTAINED AFTER EXPOSURE TO FIELD INTENSITIES OF INDICATED VALUES. THE VALUES OF POWER ABSORBED ARE ALSO INDICATED. VERTICAL SCALE 0.2 mA/ DIV; HORIZONTAL SCALE 1.0 V/DIV; 0.1 V STEP

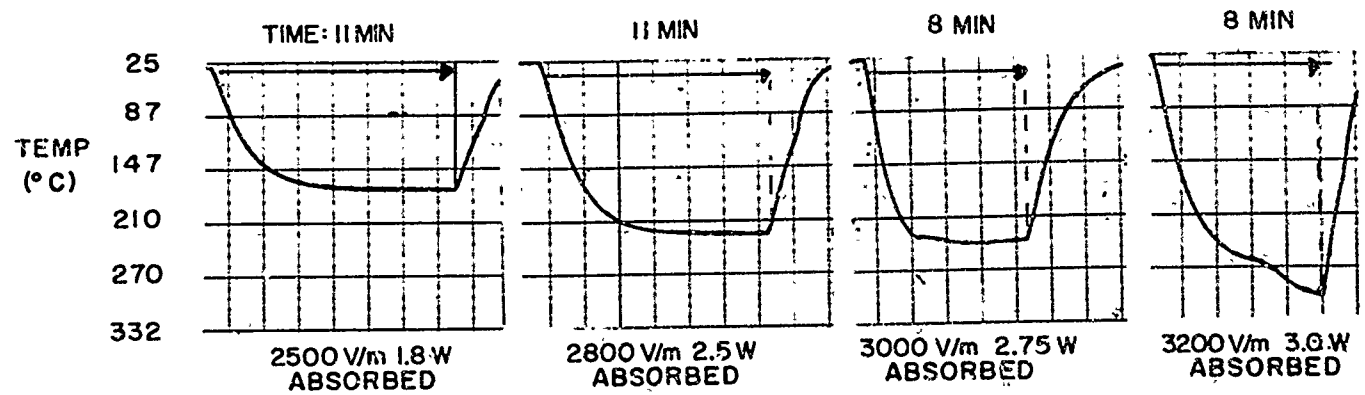

TEMPERATURE OF THE TRANSISTOR MEASURED AT THE CASE AS THE TRANSISTOR WAS EXPOSED TO rf RADIATION OF INDICATED FIELD INTENSITIES. THE VALUE OF POWER ABSORBED IS ALSO INDICATED.

Figure 36. Electrical characteristics of 2N3608 metal oxide silicon field-effect transistor (MOSFET) after exposure to EMR—transistor case TO-5; cooled by convection.

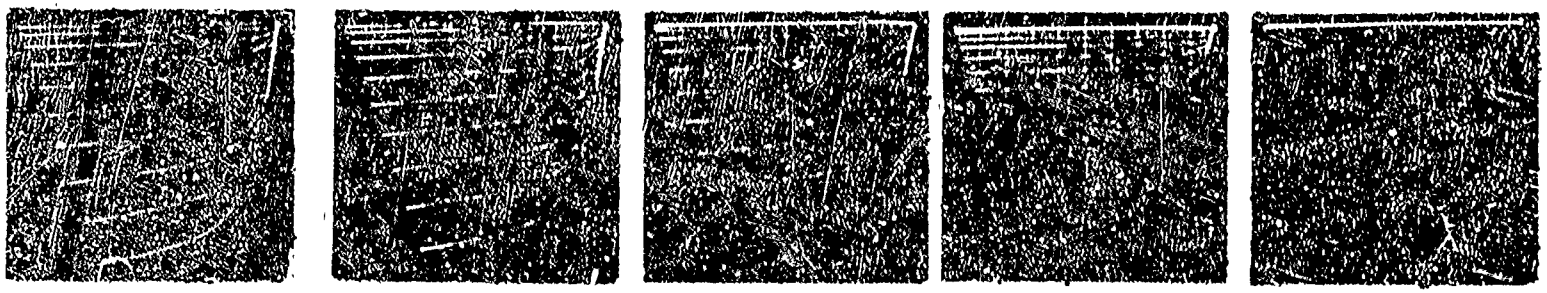

0.0 V/m 0 W ABSORBED | 1600 V/m 1.0 W ABSORBED | 1800 V/m 1.25 W ABSORBED | 1950 V/m 1.5 W ABSORBED | 2100 V/m 1.75 W ABSORBED

DRAIN CHARACTERISTICS OBTAINED AFTER EXPOSURE TO FIELD INTENSITIES OF INDICATED VALUES. THE VALUES OF POWER ABSORBED ARE ALSO INDICATED VERTICAL SCALE 0.2 mA/DIV; HORIZONTAL SCALE 1.0 V/DIV; 0.1 V STEP

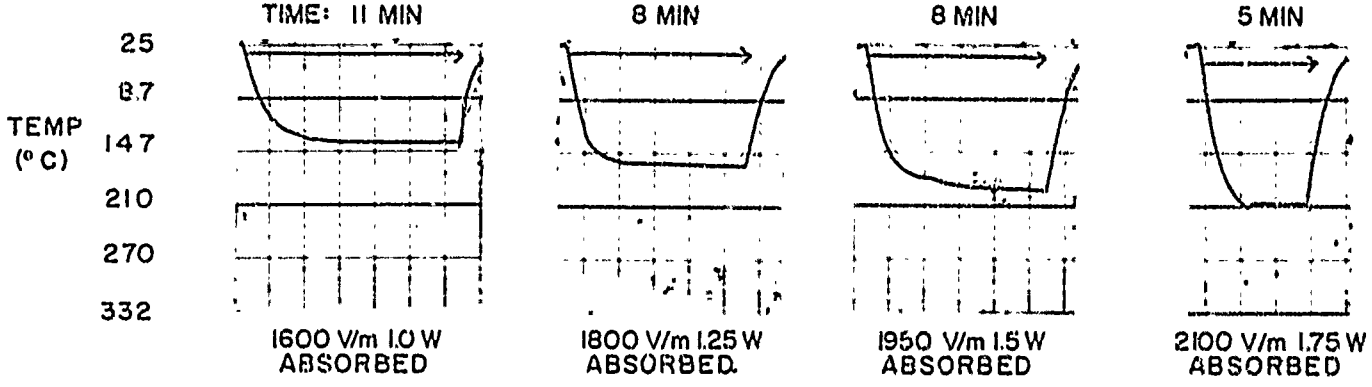

TEMPERATURE OF THE TRANSISTOR MEASURED AT THE CASE AS THE TRANSISTOR WAS EXPOSED TO rf RADIATION OF INDICATED FIELD INTENSITIES. THE VALUE OF POWER ABSORBED IS ALSO INDICATED.

Figure 37. Electrical characteristics of 2N3608 MOSFET after exposure to EMR—transistor case TO-46; cooled by convection.

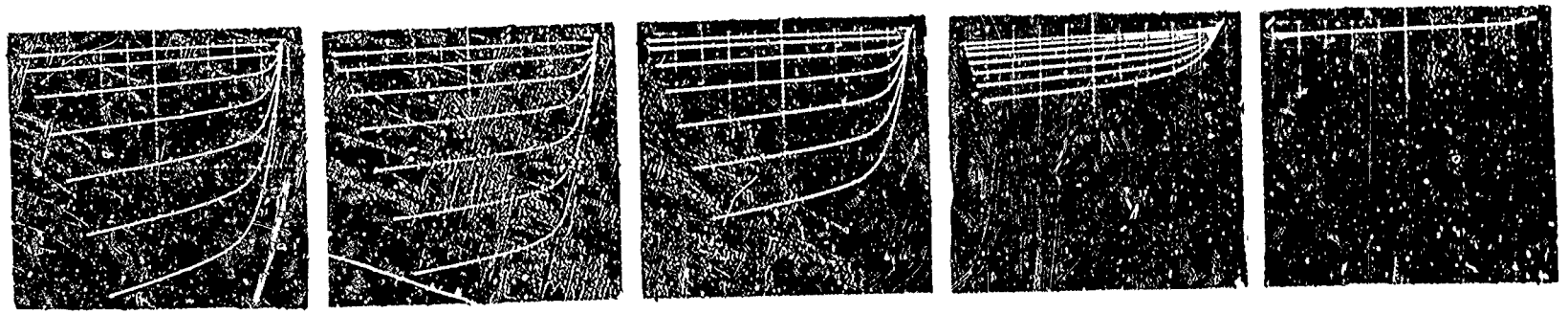

DRAIN CHARACTERISTICS OBTAINED AFTER EXPOSURE TO FIELD INTENSITIES OF INDICATED VALUES. THE VALUES OF POWER ABSORBED ARE ALSO INDICATED VERTICAL SCALE 0.2 mA/ DIV; HORIZONTAL SCALE 1.0 V/DIV; 0.1 V STEP

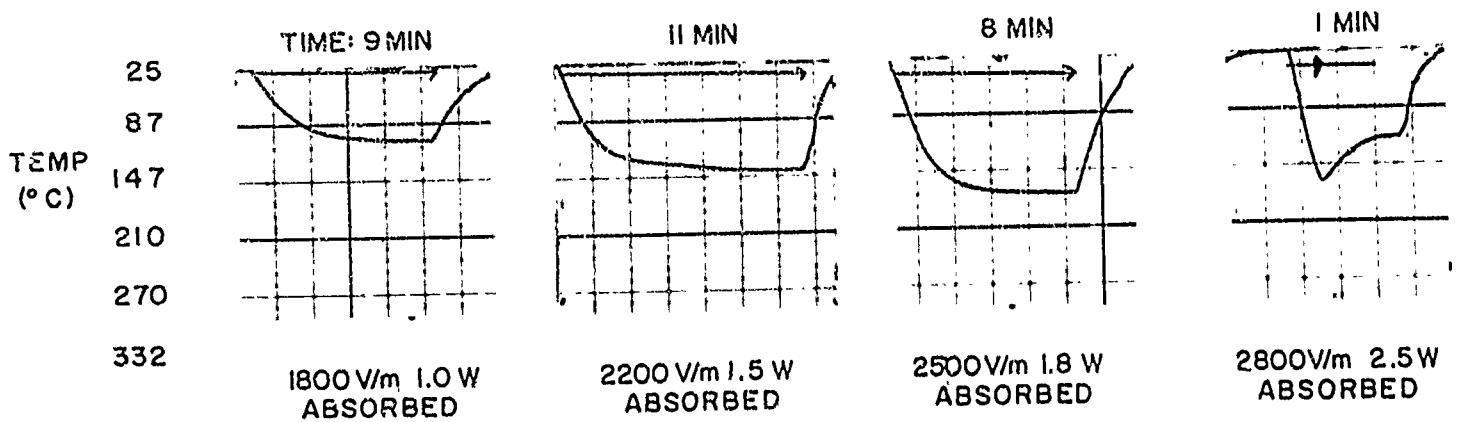

TEMPERATURE OF THE TRANSISTOR MEASURED AT THE CASE AS THE TRANSISTOR WAS EXPOSED TO rf RADIATION OF INDICATED FIELD INTENSITIES. THE VALUE OF POWER ABSORBED IS ALSO INDICATED.

Figure 38. Electrical characteristics of 2N3608 MOSFET after exposure to EMR—transistor case TO-5 removed; cooled by convection.

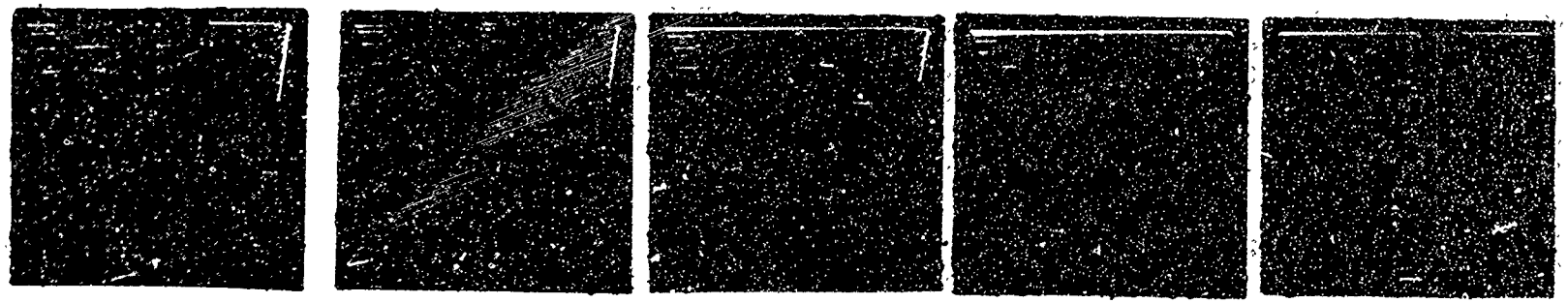

0.0 V/m 0W ABSORBED | 1000 V/m 0.5W ABSORBED | 1200 V/m 0.75 W ABSORBED | 1400 V/m 1.0W ABSORBED | 1600 V/m 1.25 W ABSORBED

DRAIN CHARACTERISTICS OBTAINED AFTER EXPOSURE TO FIELD INTENSITIES OF INDICATED VALUES. THE VALUES OF POWER ABSORBED ARE ALSO INDICATED. VERTICAL SCALE 0.2 mA/DIV; HORIZONTAL SCALE 1.0 V/DIV; 0.1 V STEP

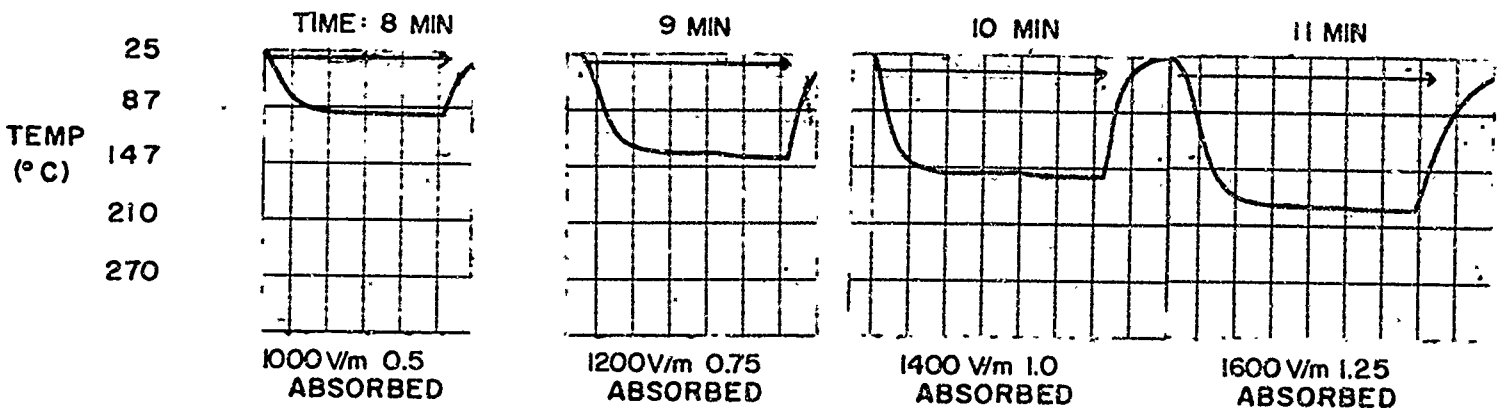

TEMPERATURE OF THE TRANSISTOR MEASURED AT THE CASE AS THE TRANSISTOR WAS EXPOSED TO rf RADIATION OF INDICATED FIELD INTENSITIES. THE VALUES OF POWER ABSORBED ARE ALSO INDICATED.

Figure 39. Electrical characteristics of 2N3608 MOSFET after exposure to EMR—transistor case TO-46 removed; cooled by convection.

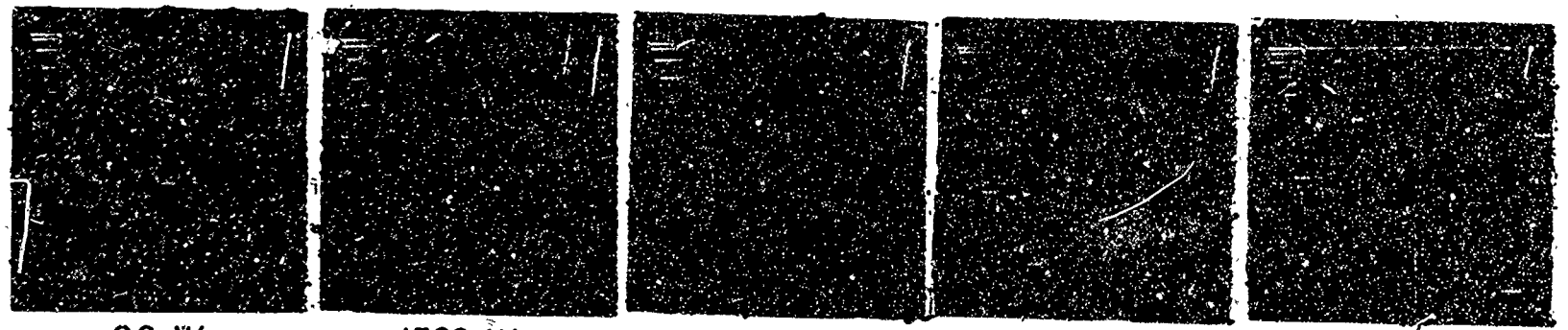

DRAIN CHARACTERISTICS OBTAINED AFTER EXPOSURE TO FIELD INTENSITIES OF INDICATED VALUES
VERTICAL SCALE 0.2 mA/DIV; HORIZONTAL SCALE 1.0 V/DIV; 0.1 V/STEP; GATE BIASED WITH 22.5 V

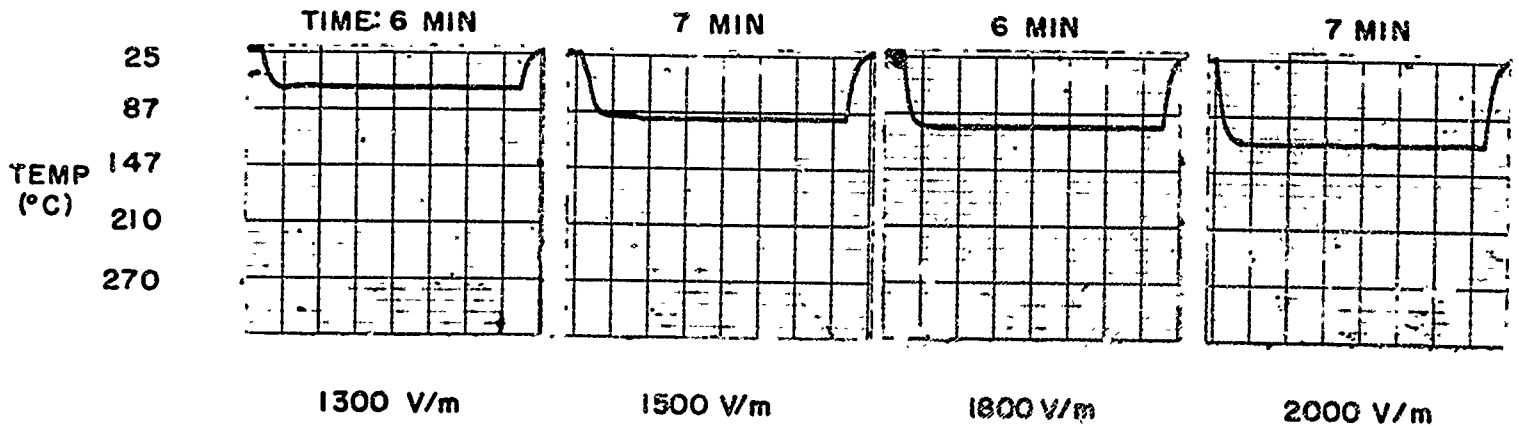

TEMPERATURE OF THE TRANSISTOR MEASURED AT THE CASE AS THE TRANSISTOR WAS EXPOSED TO rf RADIATION OF INDICATED FIELD INTENSITIES.

Figure 40. Electrical characteristics of 2N3608 MOSFET after exposure to EMR—transistor case TO-46 removed with transistor forced-air cooled.

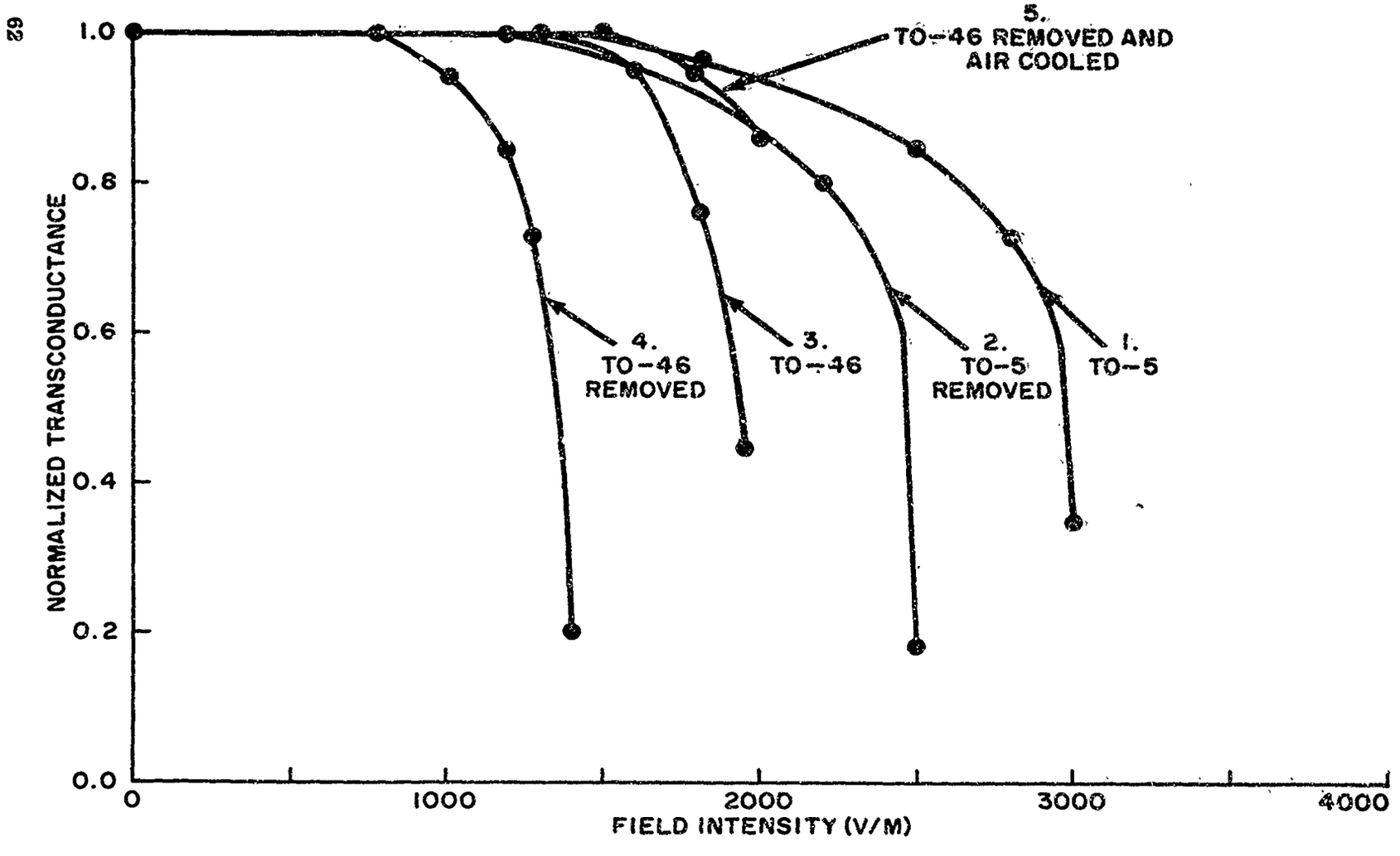

Figure 41. Normalized transconductance of 2N3608 MOSFET with applied rf field intensity for various mounting configurations.

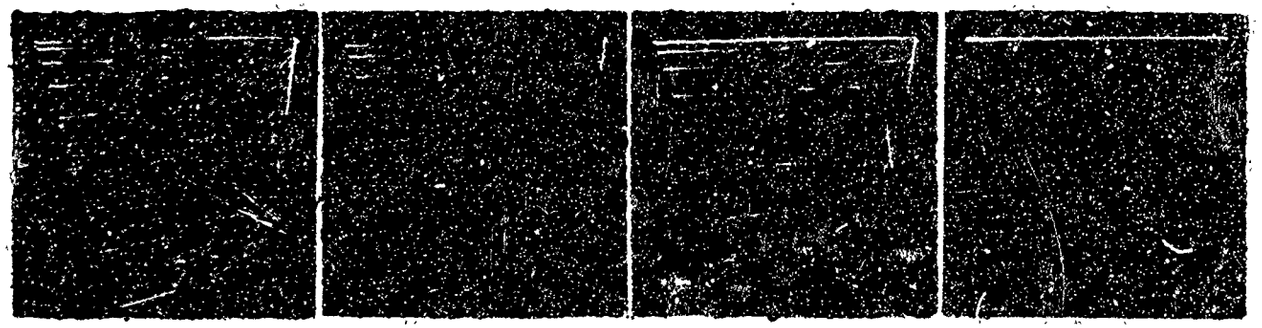

0.0 W 0.75 W 1.0 W 1.5 W

DRAIN CHARACTERISTICS OBTAINED AFTER EXPOSURE TO DC HEATING OF INDICATED VALUES OF POWER. VERTICAL SCALE 0.2 mA/DIV; HORIZONTAL SCALE 1.0 V/DIV; 0.1 STEP

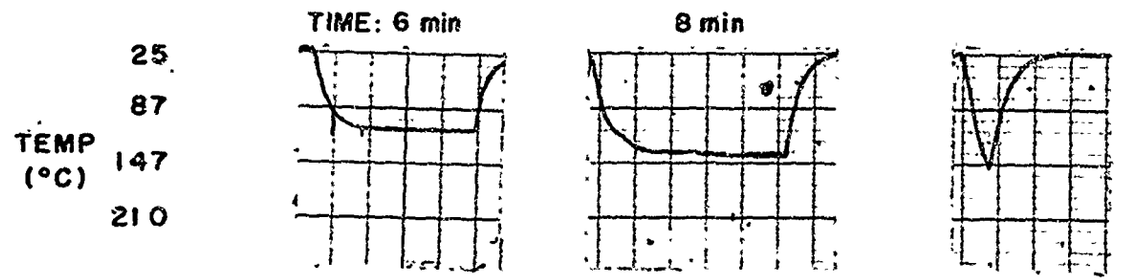

0.75 W 1.0 W 1.5 W

TEMPERATURE OF THE TRANSISTOR MEASURED AT THE CASE AS THE TRANSISTOR WAS EXPOSED TO dc HEATING OF INDICATED VALUES OF POWER

Figure 42. Electrical characteristics of 2N3608 MOSFET with d-c heating—transistor case TO-46; cooled by convection.

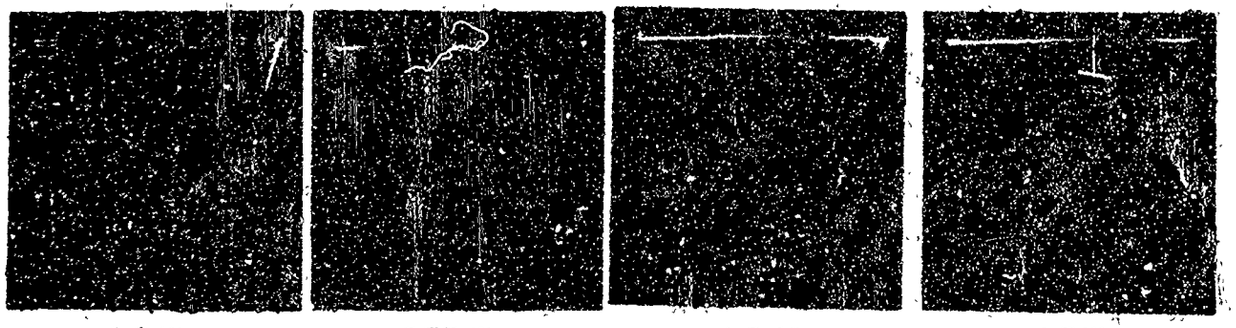

0.0 W 0.75 W 1.0 W 1.5 W

DRAIN CHARACTERISTICS OBTAINED AFTER EXPOSURE TO DC HEATING OF INDICATED VALUES OF POWER. VERTICAL SCALE 0.2 mA/DIV; HORIZONTAL SCALE 1.0 V/DIV; 0.1 STEP

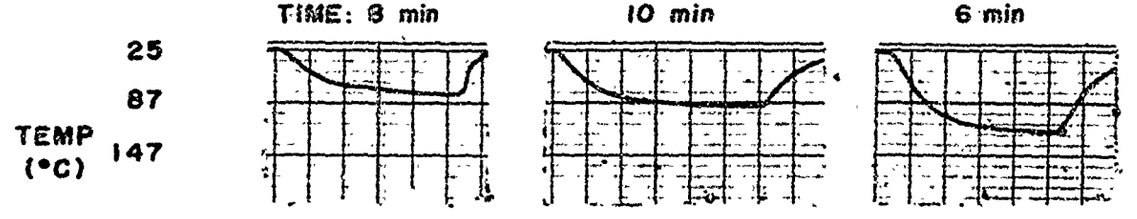

0.75 W 1.0 W 1.5 W

TEMPERATURE OF THE TRANSISTOR MEASURED AT THE CASE AS THE TRANSISTOR WAS EXPOSED TO dc HEATING OF INDICATED VALUES OF POWER

Figure 43. Electrical characteristics of 2N3608 MOSFET with d-c heating—transistor case TO-5; cooled by convection.

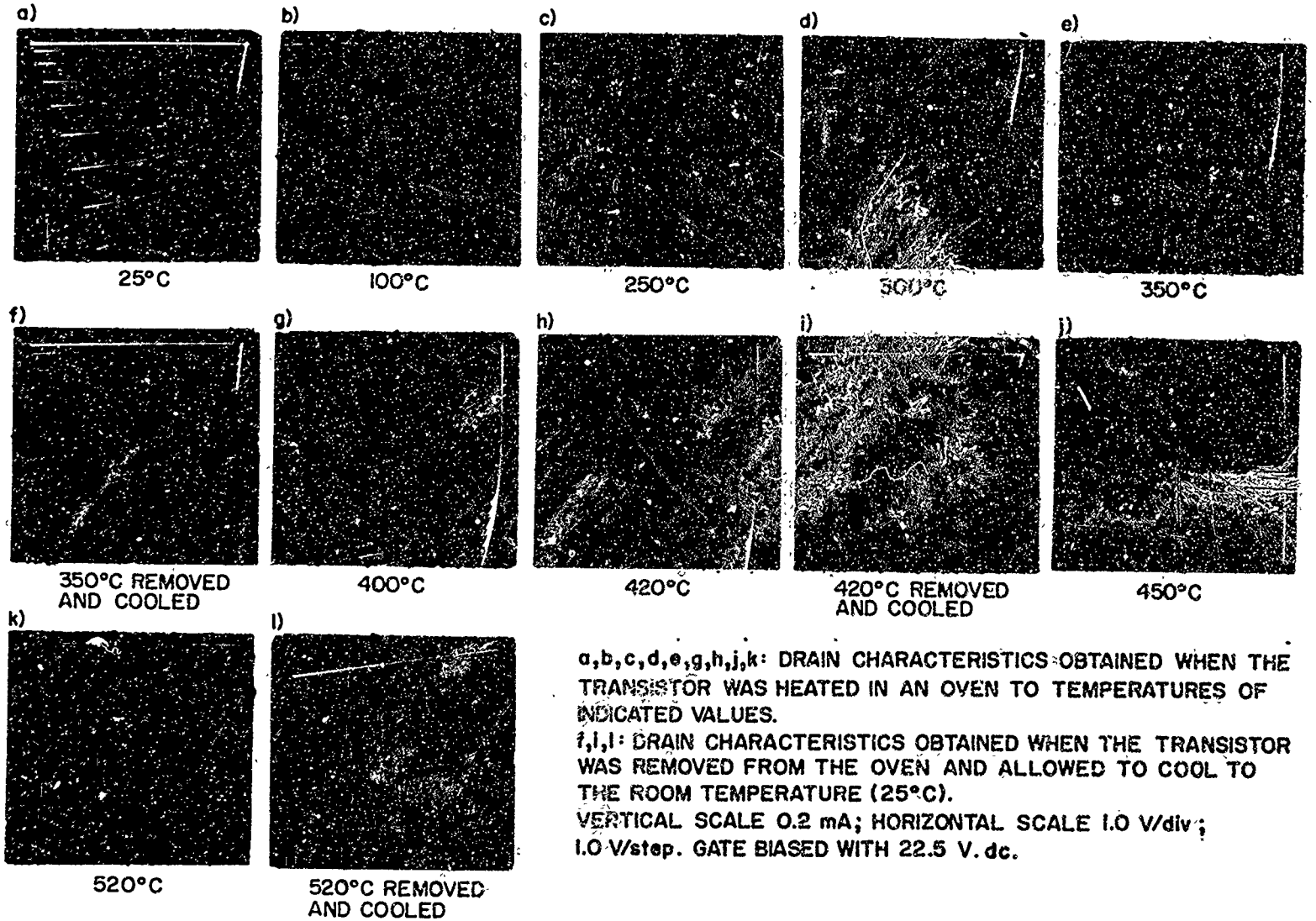

Figure 44. Electrical characteristics of 2N3608 MOSFET with temperature of indicated values in °C.

UNCLASSIFIED

Security Classification

DOCUMENT CONTROL DATA - R & D

(Security classification of title, body of abstract and indexing annotation must be entered when the overall report is classified)

1. ORIGINATING ACTIVITY (Corporate author) Harry Diamond Laboratories Washington, D. C. 20438	2a. REPORT SECURITY CLASSIFICATION UNCLASSIFIED 2b. GROUP

3. REPORT TITLE

EXPERIMENTAL INVESTIGATION OF THE PERMANENT EFFECTS OF RF RADIATION IN X-BAND ON ELECTRONIC COMPONENTS

4. DESCRIPTIVE NOTES (Type of report and inclusive dates)

5. AUTHOR(S) (First name, middle initial, last name)

Nikolai Tschursin

6. REPORT DATE June 1968	7a. TOTAL NO. OF PAGES 72	7b. NO. OF REFS 6
8a. CONTRACT OR GRANT NO. b. PROJECT NO. DA-1N022601A093 c. AMCMS Code: 5023.11.18400 d. HDL Proj. No. 24600	9a. ORIGINATOR'S REPORT NUMBER(S) TR-1399 9b. OTHER REPORT NO(S) (Any other numbers that may be assigned this report)	

10. DISTRIBUTION STATEMENT

This document has been approved for public release and sale; its distribution is unlimited.

11. SUPPLEMENTARY NOTES	12. SPONSORING MILITARY ACTIVITY AMC

13. ABSTRACT

An experimental investigation was conducted at X-band frequencies to determine the effects of rf radiation on composition resistors, crystal diodes, transistors, and metal oxide silicon field-effect transistors (MOSFET). To obtain maximum power transfer, the component leads were cut and bent to form a half-wave dipole tuned to the excitation frequency. The component was placed in a microwave assembly, oriented parallel to the electric field, and exposed for several minutes until thermal equilibrium was established.

Data concerning permanent changes in the electrical characteristics of the components as a function of exposure to the E-field were obtained. Measurements were taken of the temperature rise of the components while various types of convection and forced-air cooling were employed. These measurements indicate that the changes in the electrical characteristics of the components are primarily a function only of the temperature rise produced in the component and only secondarily if at all, a function of the field intensity per se.

DD FORM 1 NOV 65 1473 REPLACES DD FORM 1473, 1 JAN 64, WHICH IS OBSOLETE FOR ARMY USE.

UNCLASSIFIED

Security Classification

14. KEY WORDS	LINK A		LINK B		LINK C	
	ROLE	WT	ROLE	WT	ROLE	WT
RF radiation effects RF susceptibility of electronic components						